Preprints.org

Article

Not peer-reviewed version

Temporal Transcriptomic Changes in the Cingulate Cortex of Neuropathic Pain Mice

Guo-Quan Yao , Zhen-Ru Yuan , Xin-Tong Qiu , Cheng-Guo Jiang , Chong Zhang , Guang-Xi Piao , Hong Ma , Zi-He Zhu , Yu-Gang Diao * , Felipe Fregni * , Yang Bai *

Posted Date: 27 April 2026

doi: 10.20944/preprints202604.1802.v1

Keywords: neuropathic pain; cingulate cortex; transcriptomics; synaptic plasticity; neuroinflammation

Preprints.org is a free multidisciplinary platform providing preprint service that is dedicated to making early versions of research outputs permanently available and citable. Preprints posted at Preprints.org appear in Web of Science, Crossref, Google Scholar, Scilit, Europe PMC, OpenAlex.

Copyright: This open access article is published under a Creative Commons CC BY 4.0 license, which permit the free download, distribution, and reuse, provided that the author and preprint are cited in any reuse.

Preprints.org (www.preprints.org) | NOT PEER-REVIEWED | Posted: 27 April 2026 doi:10.20944/preprints202604.1802.v1

Disclaimer/Publisher's Note: The statements, opinions, and data contained in all publications are solely those of the individual author(s) and contributor(s) and not of MDPI and/or the editor(s). MDPI and/or the editor(s) disclaim responsibility for any injury to people or property resulting from any ideas, methods, instructions, or products referred to in the content.

Article

Temporal Transcriptomic Changes in the Cingulate Cortex of Neuropathic Pain Mice

Guo-Quan Yao [1,2,3], Zhen-Ru Yuan [1,2,3], Xin-Tong Qiu [4], Cheng-Guo Jiang [5], Chong Zhang [5], Guang-Xi Piao [6], Hong Ma [7], Zi-He Zhu [1,2,3], Yu-Gang Diao [1,2,3,*], Felipe Fregni [8,*] and Yang Bai [5,*]

[1] Department of Anesthesiology, General Hospital of Northern Theater Command, Shenyang, China
[2] Key Laboratory of Perioperative Critical Medicine of Liaoning Province, Shenyang, China
[3] Shenyang Clinical Medical Research Center for Anesthesiology and Perioperative Medicine, Shenyang, China
[4] Department of Anatomy, Histology and Embryology, Preclinical School of Medicine, Air Force Medical University, Xi'an, China
[5] Department of Neurosurgery, General Hospital of Northern Theater Command, Shenyang, China
[6] Department of Anesthesiology, Jilin Provincial People's Hospital, Jilin, China; 43540032@qq.com
[7] Department of Anesthesiology, First Affiliated Hospital, China Medical University, Shenyang, China
[8] Neuromodulation Center and Center for Clinical Research Learning, Spaulding Rehabilitation Hospital and Massachusetts General Hospital, Harvard Medical School, Boston, MA, USA
* Correspondence: diao72@163.com (Y.G.D.); fregni.felipe@mgh.harvard.edu (F.F.); sydbaiyang@163.com (Y.B.)

Abstract

Background: Neuropathic pain (NP), a debilitating condition from nervous system lesions, is poorly managed by current therapies. The cingulate cortex is crucial for affective pain processing, yet a comprehensive spatiotemporal understanding of its molecular changes in NP is lacking. **Methods**: This study performed RNA sequencing to profile transcriptomic alterations in the anterior cingulate (ACC) and midcingulate (MCC) cortices of mice at two and four weeks after spared nerve injury. Bioinformatics analyses, including differential expression, functional enrichment, weighted gene co-expression network analysis, and protein-protein interaction (PPI) network construction, were employed. **Results**: We identified widespread, time-dependent transcriptional dysregulation in both regions, with differentially expressed genes increasing over time. Analyses confirmed central roles for synaptic plasticity and neuroinflammatory pathways. Importantly, we uncovered significant dysregulation in proteostasis and mitochondrial function pathways, mechanisms shared with neurodegenerative diseases. PPI analysis identified stage-specific hub genes (e.g., early interferon-stimulated genes and late ribosomal proteins in ACC; persistent extracellular matrix components in MCC). **Conclusions**: This study provides a detailed transcriptomic atlas of the cingulate cortex in NP, reinforcing known mechanisms while elucidating novel dysregulation in protein homeostasis and mitochondrial pathways. The findings highlight convergent pathophysiology with neurodegeneration and offer a new theoretical framework with potential therapeutic targets for chronic NP.

Keywords: neuropathic pain; cingulate cortex; transcriptomics; synaptic plasticity; neuroinflammation

1. Introduction

Neuropathic pain (NP), a heterogeneous condition affecting roughly 10% of individuals worldwide, is defined by a lesion or disease of the somatosensory nervous system [1]. This chronic pain state imposes a profound burden on patients' quality of life and represents a persistent therapeutic challenge in clinical neurology and pain medicine [2]. First-line pharmacotherapies,

© 2026 by the author(s). Distributed under a Creative Commons CC BY license.

Preprints.org (www.preprints.org) | NOT PEER-REVIEWED | Posted: 27 April 2026 doi:10.20944/preprints202604.1802.v1

primarily comprising centrally acting drugs like opioids and certain antidepressants, often reach a therapeutic ceiling, constrained by modest efficacy and dose-limiting adverse effects [3]. This unresolved clinical predicament underscores the imperative to move beyond symptomatic management and decipher the intricate pathophysiology driving NP. A pivotal step in this direction is the comprehensive molecular profiling of pain-processing brain regions, which is expected to reveal novel mechanistic insights and unlock new, targeted therapeutic strategies [4,5]

The cingulate gyrus is a pivotal cortical hub for processing pain and emotion. It comprises four subregions—the anterior (ACC), midcingulate (MCC), posterior, and retrosplenial cortices—each defined by distinct cytoarchitecture, connectivity, and functional profiles. Among these, the ACC and MCC have been most extensively studied in the context of pain and are believed to mediate the affective dimension of pain [6,7]. Early behavioral evidence from rodent studies indicated that activation of ACC promotes behavioural sensitization and pain-related aversion [8–11]. With the advent of optogenetics for cell-specific manipulations, studies have shown that ACC glutamatergic neurons promote nociception, while GABAergic interneurons suppress it [12,13]. Circuit-level analyses indicate that the ACC integrates affective pain signals from the mediodorsal and parafascicular thalamic nuclei [14,15], and modulates pain affect via projections to mesolimbic dopamine regions, while separately regulating behavioral hypersensitivity through outputs to the spinal dorsal horn (SDH) and striatum [16–18]. Cortical long-term potentiation (LTP) in the ACC serves as a cellular model of pathological pain [19]. Nerve injury triggers lasting potentiation at excitatory synapses, involving enhanced presynaptic glutamate release and postsynaptic glutamatergic receptor recruitment [20]. Accordingly, genetic disruption of cingulate LTP alleviates NP in mice [21,22]. Recently, transcriptomic approaches have delineated ACC-wide gene expression changes in chronic pain states, confirming synaptic plasticity pathways and uncovering new roles of neuroinflammatory and apoptotic processes, thereby deepening our molecular understanding of pain pathogenesis [23–27].

The MCC is implicated in attention, cognition, emotion, and sensory processing, and its dysfunction is associated with various neurological and psychiatric disorders [28]. Human neuroimaging studies have long identified the MCC as a key hub for the perception of acute nociceptive pain [29]. Altered activity, functional connectivity, and gray matter volume within the MCC have also been reported across multiple chronic pain conditions, highlighting its vulnerability to prolonged pain states [30–32]. In rodent studies, however, the MCC was historically considered a caudal extension of the ACC and was only later recognized as a distinct cingulate subregion following the work of Vogt et al. While pain research has predominantly focused on the ACC [7], recent investigations have begun to elucidate the specific contribution of the MCC to pain modulation. Emerging evidence indicates that the MCC contributes to both sensory and affective dimensions of pain [33,34]. Specifically, the anteromedial thalamic nucleus–MCC afferent pathway mediates the transmission of nociceptive signals and associated emotional responses [35], whereas glutamatergic projections from the MCC to the zona incerta and posterior insula gate nociceptive hypersensitivity [36,37]. Despite these advances focusing on cellular mechanisms, remarkably less is known about the molecular basis underlying the neurobiology of the MCC in chronic pain.

Over the past decade, high-throughput transcriptomics has emerged as a pivotal tool in neuroscience, enabling systematic, genome-wide profiling of gene expression. This approach allows researchers to move beyond single-target studies toward a comprehensive analysis of molecular networks underlying pain mechanisms. By quantifying transcriptional changes across cell types and circuits, RNA-sequencing provides a powerful means to uncover pain-related functional adaptations in the nervous system [5,38,39]. Here, we revisit the transcriptomic landscape of the cingulate cortex to systematically characterize its temporal (two and four weeks post-modeling) and spatial (ACC and MCC subregions) dynamics in a mouse NP model induced by spared nerve injury (SNI). This approach elucidates the complex pathological reorganization within the cingulate cortex, providing an integrated perspective on its role in neuropathic pain modulation and highlighting potential therapeutic targets for intervention.

© 2026 by the author(s). Distributed under a Creative Commons CC BY license.

Preprints.org (www.preprints.org) | NOT PEER-REVIEWED | Posted: 27 April 2026 doi:10.20944/preprints202604.1802.v1

2. Materials and Methods

2.1. Animals

All animal experiments were approved by the Ethics Committee of the General Hospital of Northern Theater Command and were conducted in accordance with the National Institutes of Health Guide for the Care and Use of Laboratory Animals. Eighty-five adult male C57BL/6 mice (8 weeks old; 20–25 g) were obtained from the hospital's experimental animal department. Mice were maintained under a reversed 12 h/12 h dark/light cycle with ad libitum access to food and water.

2.2. Neuropathic Pain Model Induction and Behavioral Validation

As previously described [40], mice were deeply anesthetized and a skin incision was made in the left hind leg to expose the biceps femoris muscle. The underlying sciatic nerve and its three terminal branches—the sural, common peroneal, and tibial nerves—were then carefully isolated. Both the common peroneal and tibial nerves were tightly ligated with 6-0 silk suture and transected distal to the ligature, leaving the sural nerve intact. The muscle and skin were subsequently sutured. Sham-operated animals underwent the same surgical exposure of the sciatic nerve without ligation or transection.

Mechanical withdrawal thresholds (MWTs) of the ipsilateral hindpaw were assessed using the von Frey filament test. Prior to testing, animals were handled daily and acclimated to the testing apparatus for 30 min over three consecutive days. On test days, a series of calibrated von Frey filaments were applied perpendicularly to the plantar surface of the hindpaw. Each filament was applied five times, with each stimulus held for 5–8 s and a 5-min interval between applications. The lowest filament force that elicited at least three withdrawal responses out of five stimulations was recorded as the MWT. Positive withdrawal responses included rapid paw withdrawal, licking, shaking, or vocalization.

2.3. Study Design and Tissue Harvesting

Prior to SNI model induction, all animals were screened for baseline mechanical sensitivity of the left plantar surface using von Frey filaments. Mice exhibiting normal withdrawal thresholds (0.6, 1.0, or 1.4 g) were included, while four animals with abnormal thresholds (<0.6 g or >1.4 g) were excluded. The remaining 81 mice were randomly assigned to three groups: sham, SNI-2w, and SNI-4w. The SNI procedure was performed on the left side to induce neuropathic pain. Mechanical thresholds of the ipsilateral plantar surface were reassessed at two and four weeks post-surgery to confirm successful model establishment. Of the 54 SNI-operated animals, 52 met the success criterion (withdrawal threshold ≤0.04 g), yielding a model success rate of 96.3%. One day after the final behavioral test, mice were euthanized by rapid cervical dislocation. From each group, 24 animals were selected for cingulate cortex collection.

The cingulate cortex lies adjacent to the medial frontal cortex, regions previously shown to differentially modulate pain [9,41]. To ensure precise sampling, 300 μm coronal brain sections containing the bilateral cingulate cortex were prepared in ice-cold artificial cerebrospinal fluid (in mM: 2.6 KCl, 124 NaCl, 1 $MgCl_2$, 0.5 $CaCl_2$, 1.23 NaH_2PO_4, 26.2 $NaHCO_3$, 5 kynurenic acid, 212.7 sucrose, 10 dextrose, pH 7.4) using a vibratome, as described in prior patch-clamp studies [42,43]. Target tissues were micro-punched with a 15-gauge needle and snap-frozen on dry ice. RNA was subsequently extracted from six independent sample pools per region—ACC (bregma +1.21 to +0.13 mm) and MCC (bregma +0.01 to –0.83 mm)—each pool comprising tissue from four animals (Figure 1). To minimize RNA degradation, all tools and surfaces were treated overnight with 0.1% diethylpyrocarbonate in 0.01 M phosphate-buffered saline before use. All tissue samples were promptly stored at –80 °C. During subsequent transcriptomic processing, one ACC sample from the SNI-2w group was excluded due to suboptimal storage conditions. As a result, both this sample and its corresponding MCC sample were removed from subsequent sequencing and analysis.

© 2026 by the author(s). Distributed under a Creative Commons CC BY license.

Preprints.org (www.preprints.org) | NOT PEER-REVIEWED | Posted: 27 April 2026 doi:10.20944/preprints202604.1802.v1

Consequently, the ACC-2w and MCC-2w groups each contained five biological replicates, while all other experimental groups comprised six replicates each.

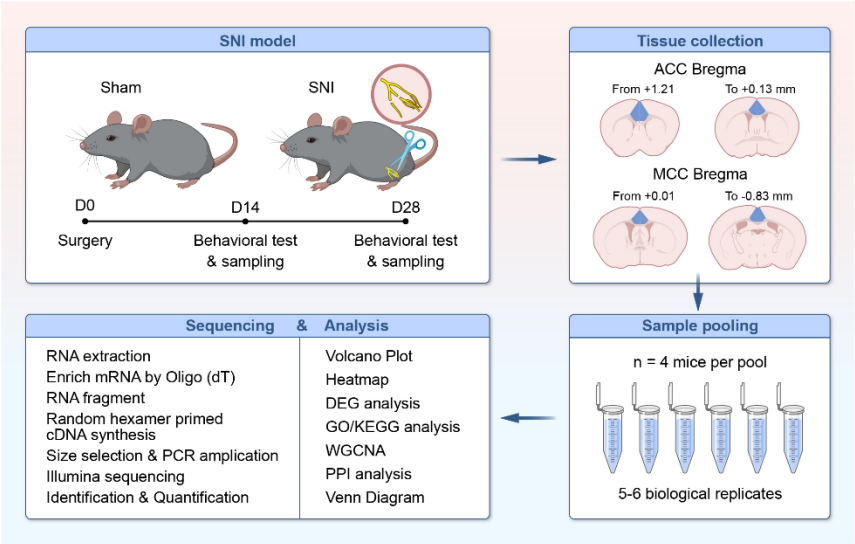

Figure 1. Systematic workflow of transcriptome analysis in the cingulate cortex of neuropathic pain mouse model.

2.4. RNA Sequencing

Total RNA was extracted from tissue samples with the TRIzol reagent (Thermo Fisher, CA, USA). The RNA quality was verified on an Agilent 5300 Bioanalyzer and quantified using a NanoDrop 2000. The construction of the sequencing library required RNA samples to meet the following quality thresholds: a total amount of 1 μg, a concentration of ≥ 30 ng/μL, an RNA Integrity Number (RIN) > 6.5, and an OD260/280 ratio between 1.8 and 2.2. mRNA was enriched from total RNA using Dynabeads Oligo (dT) (Thermo Fisher) and fragmented via incubation with divalent cations (Magnesium RNA Fragmentation Module, NEB). The resulting fragments were reverse-transcribed into cDNA using SuperScript™ II Reverse Transcriptase (Invitrogen). Second-strand cDNA synthesis was subsequently performed in the presence of dUTP to generate U-labeled DNA, utilizing a cocktail of E. coli DNA polymerase I, RNase H, and dUTP Solution (all from Thermo Fisher and NEB). Following end-repair and A-tailing, the products were ligated to dual-indexed adapters. Adapter-ligated fragments were size-selected using AMPureXP beads. The libraries were then treated with the heat-labile UDG enzyme (NEB) to digest the U-labeled strand prior to PCR amplification. The PCR was carried out under the following conditions: 95 °C for 3 min; 8 cycles of 98 °C for 15 s, 60 °C for 15 s, and 72 °C for 30 s; with a final extension at 72 °C for 5 min. The resulting cDNA libraries, with an average insert size of 300 ± 50 bp, were sequenced on an Illumina NovaSeq X Plus platform for 2×150 bp paired-end reads.

2.5. Transcriptomic Analysis

RNA sequencing yielded 845.17 million paired-end reads (2 × 150 bp). Raw reads were processed with Fastp (v0.22.0) to remove adapter sequences and low-quality bases, followed by quality assessment using FastQC (v0.11.9). After quality control, 252.10 Gb of clean reads were retained and aligned to the mouse reference genome using HISAT2 (v 2.2.1). Gene-level read counts were obtained using featureCounts (v2.0.1). Raw counts were transformed to log2 counts per million [$\log_2$(CPM + 1)] using the cpm function in the edgeR package (v4.4.0) for downstream expression analyses. Specifically, $\log_2$CPM values were calculated as $\log_2$(CPM + 1) to stabilize variance and avoid taking the logarithm of zero. PCA was performed on the scaled expression matrix using the PCA function

© 2026 by the author(s). Distributed under a Creative Commons CC BY license.

Preprints.org (www.preprints.org) | NOT PEER-REVIEWED | Posted: 27 April 2026 doi:10.20944/preprints202604.1802.v1

from the FactoMineR package (v2.11) in R. The first two principal components were visualized with the fviz_pca_ind function from the factoextra package (v1.0.7), with samples colored according to experimental group. Differential expression analysis was performed with DESeq2 (v1.48.1), applying thresholds of |fold change (FC)| > 1.5 and adjust p-value (padj) < 0.05 to define DEGs. Venn diagrams were generated using ggVennDiagram (version 1.5.3) in R/Bioconductor. Functional enrichment analysis of DEGs for GO terms and KEGG pathways was carried out using the clusterProfiler R package (v4.16.0).

To construct the co-expression network, we employed the WGCNA package (version 1.73) to calculate similarity between gene expression profiles [44]. A scale-free network was built using the WGCNA method. The adjacency matrix was converted into a topological overlap matrix through hierarchical clustering, and different modules were identified by applying a dynamic tree-cut algorithm. Parameter settings were as follows: the minimum number of genes per module was set to 50 (minModuleSize = 50); the threshold for reassigning genes between modules was set to False (pamRespectsDendro = FALSE); and the cut-height for merging modules was set to 0.3 (cutHeight = 0.3).

To investigate functional connectivity among DEGs, protein–protein interactions between significant DEGs across cingulate subregions and time points were predicted using the STRING database (v12.0) [45], with the minimum required interaction score set to "high confidence" (0.7) and disconnected nodes hidden from the network visualization. The cytoHubba's Maximal Clique Centrality score was used to identify top hub DEGs and their sub-networks. The data were visualized using Cytoscape (v3.7.0)[23].

3. Results

3.1. Overview of RNA-seq Data and Basic Alignment Metrics

Transcriptome profiling of cingulate cortex subregions was performed via RNA sequencing at 14 and 28 days following SNI or sham surgery (Figure 1). After quality control, an average of 24,659,123 clean reads per sample were obtained from approximately 25 million raw reads and aligned to the reference genome with a mapping rate of 98.5–99.0% (Table A1). Detected genes were quantified and their distribution across samples is summarized in Figure A1a–b. To assess experimental consistency and sample suitability, we evaluated inter-sample correlations based on normalized expression values, as visualized in the correlation heatmap (Figure A1c).

3.2. Altered Transcriptional Signatures in the Cingulate Cortex After SNI

We next examined the expression profiles of differentially expressed genes (DEGs) in cingulate subregions following SNI. Transcriptome-wide sequencing detected approximately 37,536 and 37,861 expressed genes in the ACC and MCC, respectively, at two weeks post-SNI, followed by 38,103 and 38,985 genes at four weeks. Principal component analysis (PCA) revealed clear separation among the six experimental groups, indicating distinct transcriptional patterns among the groups (Figure 2a). The number of altered genes increased with longer post-injury intervals. In the ACC, volcano plot analysis identified 63 up- and 62 down-regulated genes at 2 weeks post-SNI, and 195 up- and 384 down-regulated genes at 4 weeks, compared with sham controls (Figure 2b-c). Correspondingly, in the MCC we detected 93 up- and 18 down-regulated genes at 2 weeks, and 309 up- and 52 down-regulated genes at 4 weeks (Figure 3a-b). A heatmap of the top 40 DEGs (ranked by padj) further confirmed clear segregation between experimental and control groups (Figure 2d-e and 3c-d). Across both regions and time points, protein-coding RNAs accounted for the majority of transcriptional changes (81.8-94.4%), followed by long non-coding RNAs (4.7-10.8%) and pseudogenes (0.9-6.5%) (Figure A1d).

© 2026 by the author(s). Distributed under a Creative Commons CC BY license.

Preprints.org (www.preprints.org) | NOT PEER-REVIEWED | Posted: 27 April 2026 doi:10.20944/preprints202604.1802.v1

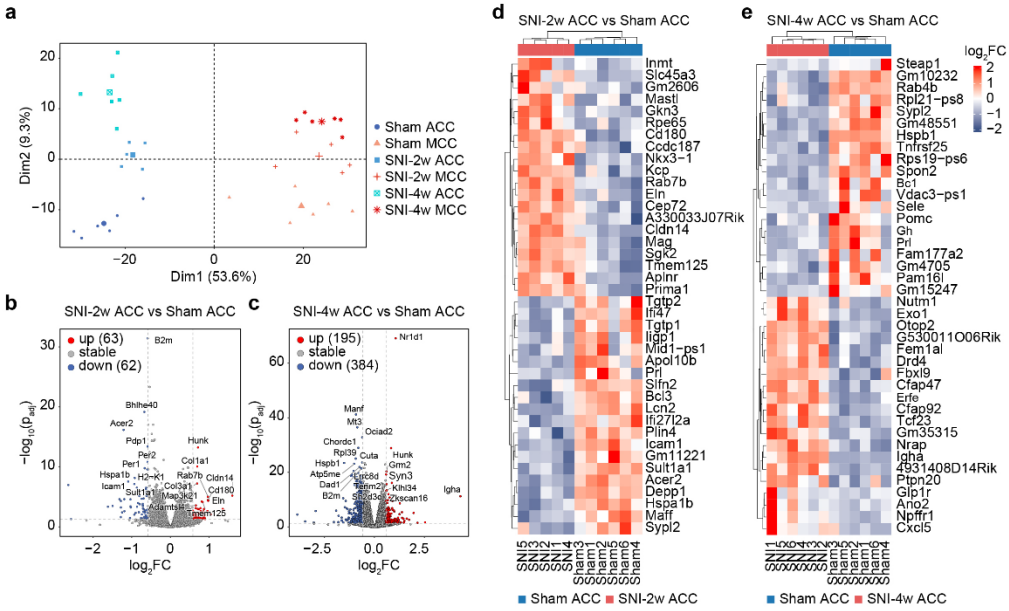

Figure 2. General transcriptomic outcomes of ACC. **a** Principal component analysis indicated a near complete separation of genes among these six groups. **b-c** Volcano plots of DEGs in SNI-2w (b) and SNI-4w (c) group compared to sham group. The red and blue dots indicate significantly up-regulated and down-regulated genes, respectively. **d-e** Hierarchical cluster analysis of SNI-2w (d) and SNI-4w (e) group compared to sham group. Red indicates up-regulation, and blue indicates down-regulation. The dendrograms represent the classification of genes. The number in the color scale indicates the Log2 fold change values (Log2FC).

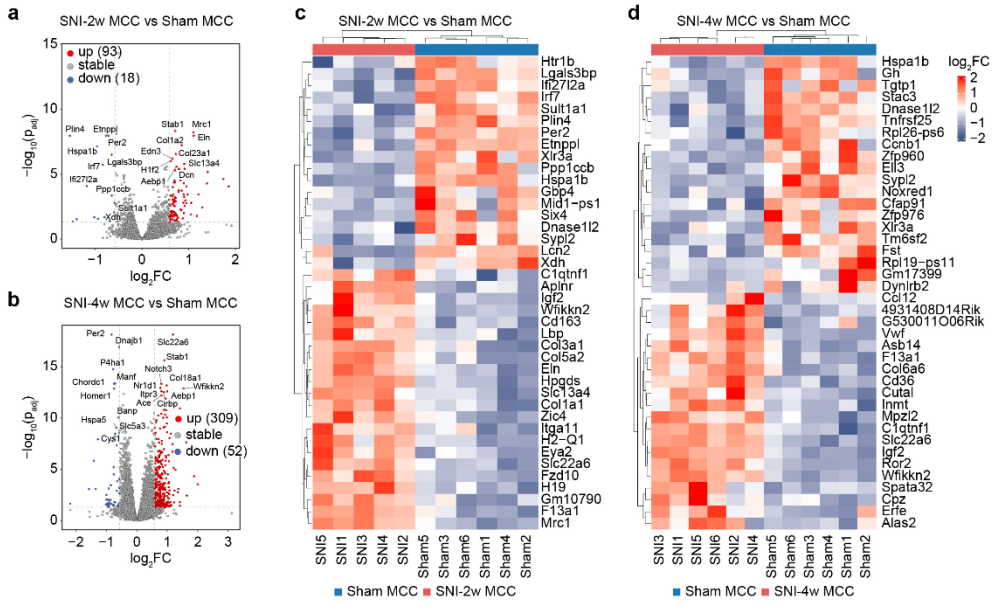

Figure 3. General transcriptomic outcomes of MCC. **a-b** Volcano plots of DEGs in SNI-2w (a) and SNI-4w (b) group compared to sham group. The red and blue dots indicate significantly up-regulated and down-regulated genes, respectively. **c-d** Hierarchical cluster analysis of SNI-2w (c) and SNI-4w (d) group compared to sham group. Red indicates up-regulation, and blue indicates down-regulation. The dendrograms represent the classification of genes. The number in the color scale indicates the Log2 fold change values (Log2FC).

Synapse-related molecules, G protein-coupled receptors (GPCRs), ion channels, and neuropeptides play critical roles in the transmission and modulation of nociceptive signals [46–48]. Based on prior annotations [49,50], we curated a reference set of genes (Table A2) within these

© 2026 by the author(s). Distributed under a Creative Commons CC BY license.

Preprints.org (www.preprints.org) | NOT PEER-REVIEWED | Posted: 27 April 2026 doi:10.20944/preprints202604.1802.v1

functional categories and cross-referenced them with our DEGs. This analysis revealed a notable enrichment of DEGs encoding GPCRs, followed by neuropeptides, and a few synapse-associated molecules, whereas no significant changes were observed in ion channels (Figure 4a). Among the altered neuropeptides, we detected differential expression of *Npy*—which is known to modulate pain at both spinal and supraspinal levels [51,52]—and *Prok2*, previously implicated in neuropathic pain and negative affect via the nucleus accumbens shell [53]. Within the GPCR category, several receptors with established roles in pain processing showed altered expression, including the class A GPCRs *Mc4r* [54] and *Htr1b* [55], the G protein-coupled estrogen receptor *Gper1*[56], and the class C metabotropic glutamate receptor *Grm2*[57]. Although not previously linked directly to pain, *Baiap3*—a gene implicated in dense-core vesicle trafficking and post-synaptic neurotransmission deficits—has been shown to regulate depressive-like behaviors in the prefrontal cortex[58].

Emerging evidence underscores the role of transcription factors (TFs) in chronic pain [59–61]. In this study, we identified a broader repertoire of TFs with altered expression in the cingulate cortex under NP conditions (Figure 4b). These include: *Bcl3*, an atypical IκB family protein that modulates NF-κB activity [62]; *Irf7*, a member of the interferon regulatory factor family [63]; *Hipk2*, an evolutionarily conserved serine/threonine kinase involved in neuronal development and homeostasis [64]; and *Tfap2b*, an AP-2 family transcription factor implicated in organ development and differentiation [65]. All four have been linked to pain regulation in the spinal cord via neuroinflammatory mechanisms [63,66–68]. Notably, *Bcl3* and *Irf7* were down-regulated in the NP model, whereas *Hipk2* and *Tfap2b* were up-regulated. Additionally, we observed upregulation of *Adnp*, a key factor in brain formation and function. Although not previously associated directly with pain, ADNP has been shown to modulate synaptic plasticity in ACC neurons through Wnt signaling and to counteract anesthesia-induced social and cognitive deficits [69].

Broad transcriptional changes are often associated with extensive chromatin remodeling and epigenetic regulation. Among the 720 known epigenetic regulators [70], we observed altered expression of a limited set of genes implicated in histone modification when comparing sham and SNI mice across cingulate subregions (Figure 4c). These include *Banp* and *Srcap*, involved in histone acetylation; *Kdm4d* and *Prdm6*, associated with histone methylation; *Eya2* and *Mastl*, linked to histone phosphorylation; as well as *Hspa1a* and *Hspa1b*, which participate in histone acetylation, methylation, and ubiquitination. Notably, both *Hspa1a* and *Hspa1b*—which encode members of the heat shock protein family A—participate in pain modulation. While Hspa1a counteracts inflammatory pain by suppressing macrophage glycolysis, Hspa1b may promote NP through endoplasmic reticulum stress-related mechanisms at the level of the SDH [71,72].

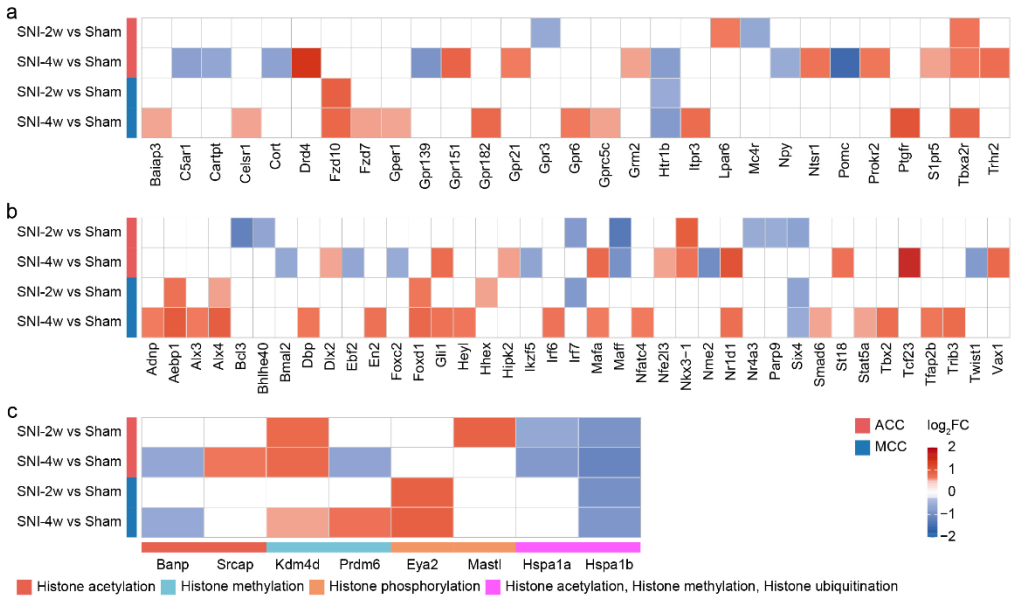

© 2026 by the author(s). Distributed under a Creative Commons CC BY license.

Preprints.org (www.preprints.org) | NOT PEER-REVIEWED | Posted: 27 April 2026 doi:10.20944/preprints202604.1802.v1

Figure 4. Heatmaps of the representative DEGs in the cingulate cortex after nerve injury. **a-c** DEGs of synapse-related molecules, G protein-coupled receptors, ion channels, neuropeptides (a), transcription factors (b), and epigenetic regulators (c) in the cingulate cortex after nerve injury. Colors in the heatmaps indicate the Log2 fold change values (Log2FC) among the different datasets. The up- and down-regulated genes are colored in red and blue, respectively. Under panel c, the bottom-row annotation designates the functional categories of epigenetic modifiers.

3.3. Functional Enrichment Analysis of the Differentially Expressed Genes After SNI

To elucidate the functional implications of the identified DEGs, we performed Kyoto Encyclopedia of Genes and Genomes (KEGG) pathway enrichment analysis, with key results presented in Figure 5. In the MCC, DEGs from both the 2- and 4-week post-SNI groups were enriched in pathways related to Protein digestion and absorption, Extracellular matrix (ECM)-receptor interaction, and Phosphoinositide 3-kinase–protein kinase B (PI3K-Akt) signaling pathway. Additionally, the SNI-4w group showed specific enrichment in the Transforming growth factor-beta (TGF-beta) signaling pathway, Hippo signaling pathway, and Circadian rhythm. In the ACC, DEGs from both time points were commonly enriched in Circadian rhythm and Neuroactive ligand-receptor interaction. The SNI-2w group further displayed enrichment in Protein digestion and absorption, Tumor necrosis factor (TNF) signaling pathway, Nuclear factor kappa B (NF-κB) signaling pathway, and Mitogen-activated protein kinase (MAPK) signaling pathway, whereas the 4-week group was distinctly enriched in Chemical carcinogenesis—reactive oxygen species, Retrograde endocannabinoid signaling, and Pathways of neurodegeneration—multiple disease.

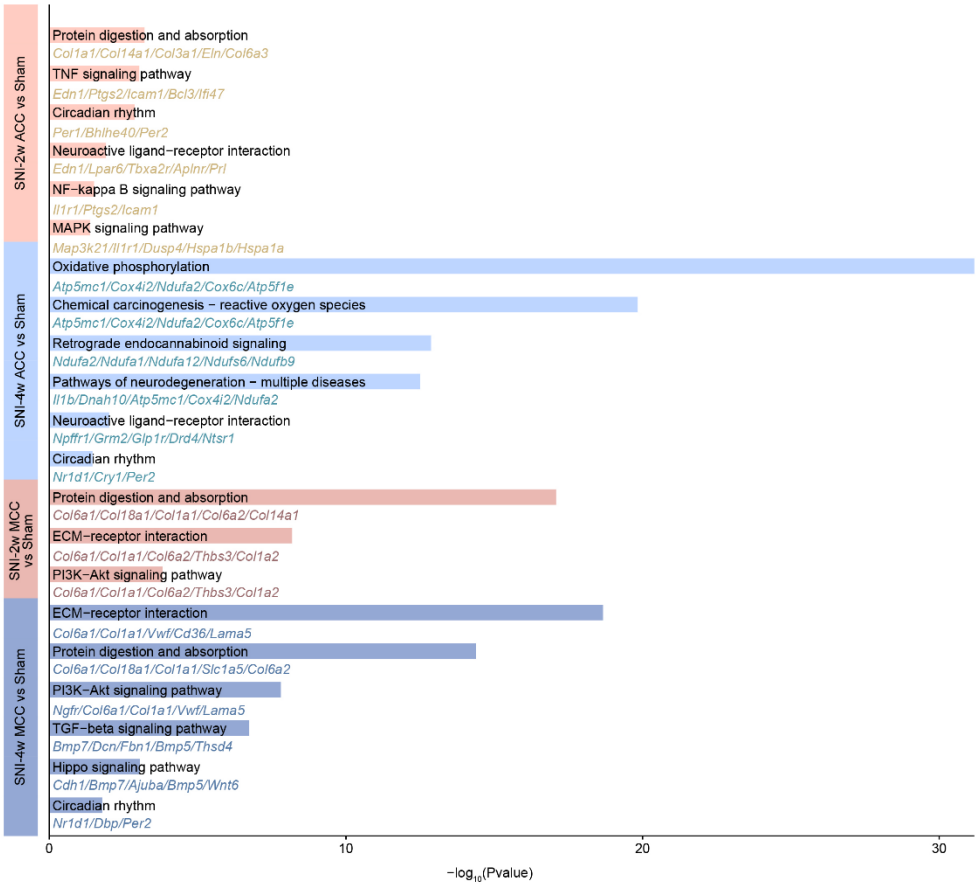

Figure 5. Bar plot showing the KEGG term analysis results of the DEGs.

© 2026 by the author(s). Distributed under a Creative Commons CC BY license.

Preprints.org (www.preprints.org) | NOT PEER-REVIEWED | Posted: 27 April 2026 doi:10.20944/preprints202604.1802.v1

To complement our KEGG analysis of DEGs, we next constructed Weighted Gene Co-expression Network Analysis (WGCNA) networks for the ACC and MCC (Figure 6 and Figure A2). For network construction, a soft-thresholding power (β) of 3 was selected to achieve a scale-free topology fit ($R^2 > 0.8$). Modules were identified using topological overlap matrices with a dynamic tree-cutting algorithm, setting a minimum module size of 50 genes. Modules with high similarity (cut height = 0.3) were merged, yielding 38 distinct co-expression modules in the ACC (module size range: 52 genes in 'darkolivegreen' to 4,272 genes in 'darkred'; Figure 6a) and 22 modules in the MCC (module size range: 56 genes in 'indianred3' to 3,199 genes in 'blue2'; Figure 6e). To explore the biological relevance of ACC-associated modules, we correlated module eigengenes (MEs) with experimental groups. Several modules showed significant associations with NP states (Figure 6a–b). The plum1 module was positively correlated with the sham group ($r = 0.72$, $p < 0.01$), whereas navajowhite1 correlated with the SNI-2w group ($r = 0.50$, $p < 0.05$). The darkred module showed a strong positive correlation with the SNI-4w group ($r = 0.88$, $p < 0.0001$). These three modules were therefore selected for further enrichment analysis. KEGG and Gene Ontology (GO) biological process analyses revealed that plum1 was enriched for pathways related to oxidative phosphorylation, including Proteasome, Protein processing in endoplasmic reticulum, and Pathways of neurodegeneration—multiple diseases; Navajowhite1 was enriched in immune-response pathways such as ECM–receptor interaction, PI3K–Akt signaling, and NF-κB signaling; Darkred was associated with synaptic structure and function, including Glutamatergic synapse, Calcium signaling, and cyclic adenosine monophosphate (cAMP) signaling pathways (Figure 6c–d).

Similarly, in the MCC, three key modules were identified based on significant correlations with experimental groups (Figure 6e–f). The darkturquoise module was positively correlated with the sham group ($r = 0.79$, $p < 0.001$), darkseagreen3 with SNI-2w ($r = 0.49$, $p < 0.05$), and darkviolet with SNI-4w ($r = 0.73$, $p < 0.001$). Enrichment analysis showed that darkturquoise was associated with protein-folding pathways including Autophagy, Protein processing in endoplasmic reticulum, and Pathways of neurodegeneration—multiple diseases; Darkseagreen3 was enriched in axon ensheathment-related terms such as ether lipid metabolism, sphingolipid metabolism, and Fatty acid metabolism; Darkviolet was linked to ECM organization, involving PI3K–Akt signaling, TGF-β signaling, and ECM–receptor interaction (Figure 6g–h). Collectively, the WGCNA results substantiate the preceding KEGG pathway analysis, underscoring the pivotal roles of synaptic transmission/plasticity and neuroinflammatory mechanisms in the pathophysiology of NP. Furthermore, these findings suggest that NP may share underlying pathological mechanisms, such as proteostasis disruption and mitochondrial dysfunction, with various neurodegenerative disorders.

© 2026 by the author(s). Distributed under a Creative Commons CC BY license.

Preprints.org (www.preprints.org) | NOT PEER-REVIEWED | Posted: 27 April 2026 doi:10.20944/preprints202604.1802.v1

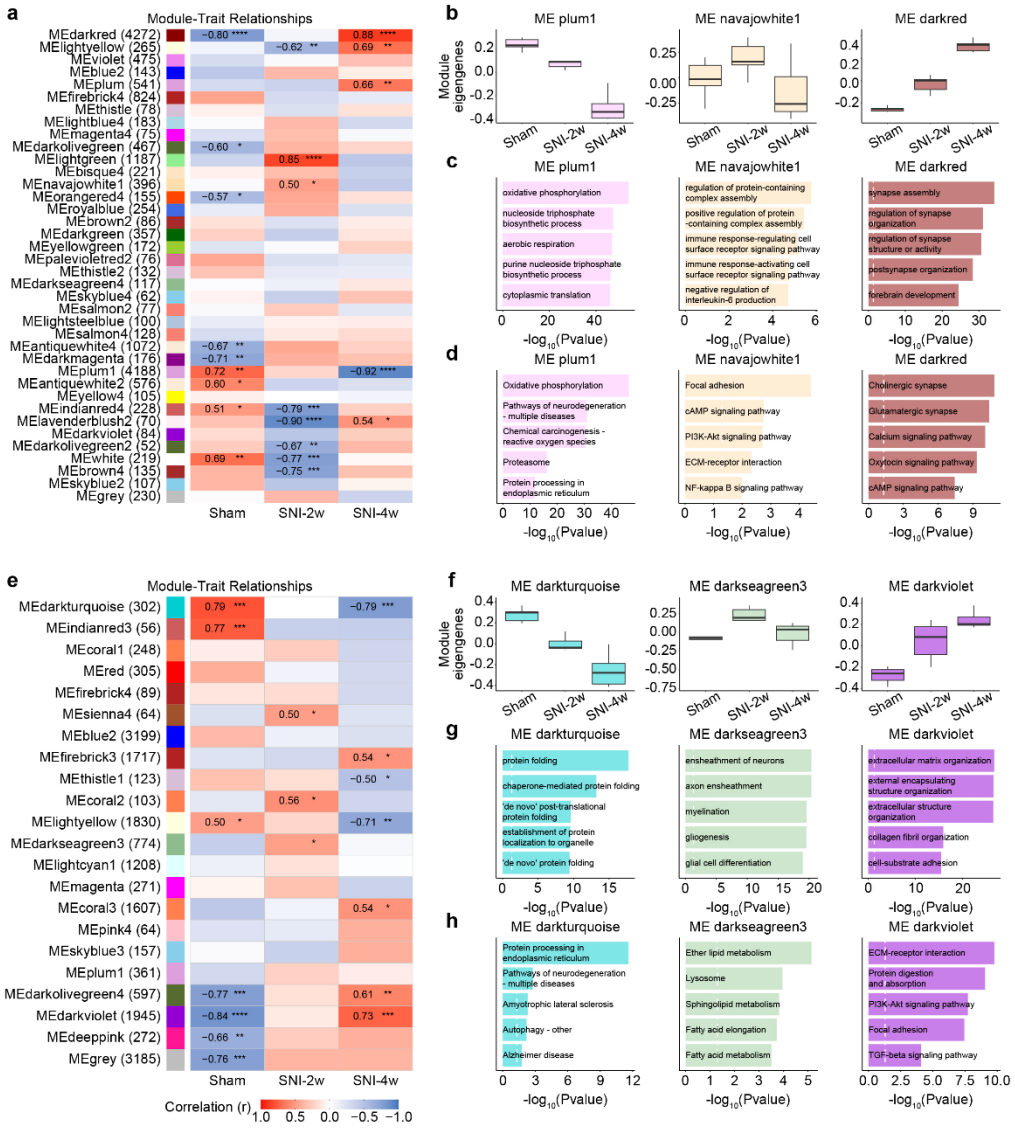

Figure 6. WGCNA analysis. **a** Correlation analysis between gene modules and phenotypes in the ACC. The heatmap presents correlation coefficients and associated p-values between each gene co-expression module and the phenotypic groups (sham, SNI-2w, and SNI-4w). Positive ($r > 0$) and negative ($r < 0$) correlations indicate, respectively, up- or down-regulated co-expression patterns for each module in a given group, and color intensity denotes the strength of the correlation. * indicates p value < 0.05 for NP trait, ** indicates p value < 0.01, *** indicates p value < 0.001, and **** indicates p value < 0.0001. **b** Boxplots showing the distribution of module expression (mean $\log_2$CPM of all genes within a given module) for different groups. **c-d** Enrichment analysis of the three selected module. Representative enriched biological process terms and KEGG pathways for each module are displayed in c and d, respectively. The left panels correspond to the sham group, the middle panels to the SNI-2w group, and the right panels to the SNI-4w group. **e-h** WGCNA network in the MCC. The conventions are the same as those in a-d.

3.4. Protein-Protein Interaction Analysis After SNI

To investigate the molecular interactions and identify potential key drivers among the DEGs in the ACC and MCC following SNI, we conducted a PPI network analysis using the STRING database. In the ACC, the DEG network comprised 36 nodes with 90 edges in the SNI-2w group and 188 nodes with 2042 edges in the SNI-4w group. Among the top 10 hub genes in the SNI-2w group, the majority were interferon-stimulated genes encoding GTPase-active proteins (e.g., *Ifi47*, *Gbp2*, *Ifi44*, *Iigp1*, *Igtp*) along with core structural components of the ECM (*Col1a1* and *Col3a1*). In contrast, the top 10 hub

© 2026 by the author(s). Distributed under a Creative Commons CC BY license.

Preprints.org (www.preprints.org) | NOT PEER-REVIEWED | Posted: 27 April 2026 doi:10.20944/preprints202604.1802.v1

genes in the SNI-4w group were exclusively ribosomal protein genes (Figure 7a–b). While recent studies have implicated interferon signaling in ACC-mediated neuroinflammation [73,74] and ECM remodeling in synaptic plasticity [75,76] during chronic pain, the functional role of ribosomal proteins in pain pathogenesis remains largely unexplored. Similarly, in the MCC, network analysis revealed 45 nodes with 188 edges in the SNI-2w group and 225 nodes with 1796 edges in the SNI-4w group. Notably, the top 10 hub DEGs in both the 2-week and 4-week MCC networks were predominantly essential constituents of the ECM (Figure 7c–d). These findings collectively suggest that dysregulation of ECM organization within the cingulate cortex may represent a pivotal mechanism underlying the pathological progression of NP.

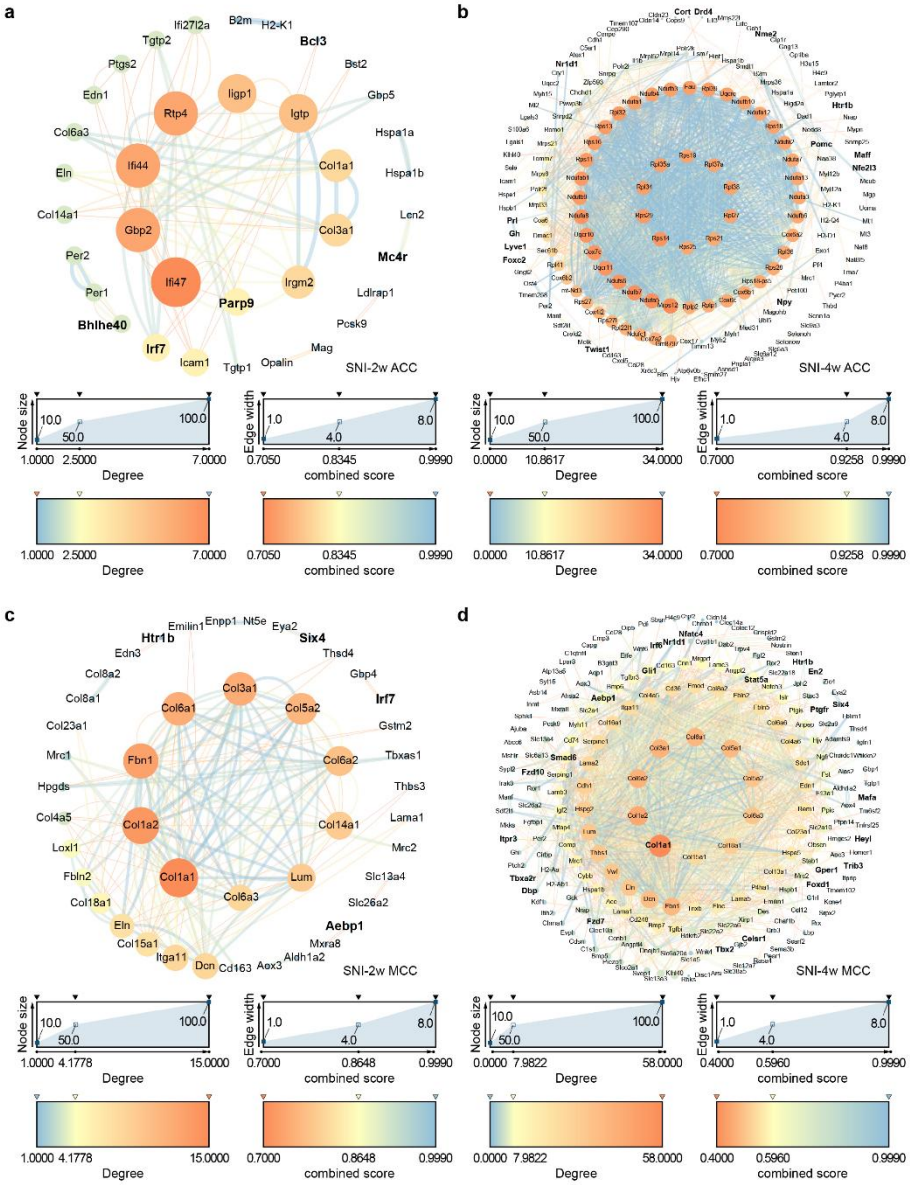

Figure 7. PPI networks of the DEGs in SNI groups comparing the sham group. **a-b** STRING PPI networks illustrating potential interactions among DEGs in the ACC at 2 weeks (a) and 4 weeks (b) post-SNI. **c-d** STRING PPI networks illustrating potential interactions among DEGs in the MCC at 2 weeks (c) and 4 weeks (d) post-SNI. Node color and size correspond to the degree of connectivity; edge color and thickness correspond to the combined interaction score. Central nodes (hub genes) represent the top 10 DEGs ranked by connectivity degree, while peripheral nodes denote other DEGs with predicted interactions. Bold labels in the panels indicate genes categorized as synapse-related molecules, G protein-coupled receptors, ion channels, neuropeptides, or transcription factors.

© 2026 by the author(s). Distributed under a Creative Commons CC BY license.

Preprints.org (www.preprints.org) | NOT PEER-REVIEWED | Posted: 27 April 2026 doi:10.20944/preprints202604.1802.v1

3.5. Shared Transcriptional Changes in Cingulate Subregions Across Time Points

By integrating all transcriptomic datasets and conducting Venn diagram analysis, we identified seven overlapping targets (Figure 8). Among these, four genes—*Cd180* (encoding CD180 antigen), *Map3k21* (encoding mitogen-activated protein kinase kinase kinase 21), *Cldn14* (encoding claudin-14), and *2410022M11Rik* (a functionally uncharacterized non-coding RNA)—were consistently up-regulated across different post-injury time points and subregions of the cingulate cortex following SNI. Conversely, three genes—*Sypl2* (encoding synaptophysin-like 2), *Per2* (encoding period circadian regulator 2), and *Hspa1b* (encoding heat shock protein family A member 1B)—showed consistent down-regulation under the same conditions. In prior KEGG pathway analysis, *Per2* was enriched in the circadian rhythm pathway, while *Hspa1b* and *Map3k21* were enriched in the MAPK signaling pathway (Figure 5). Notably, Per2 has been previously demonstrated to contribute to NP via neuroinflammatory mechanisms within the SDH [77].

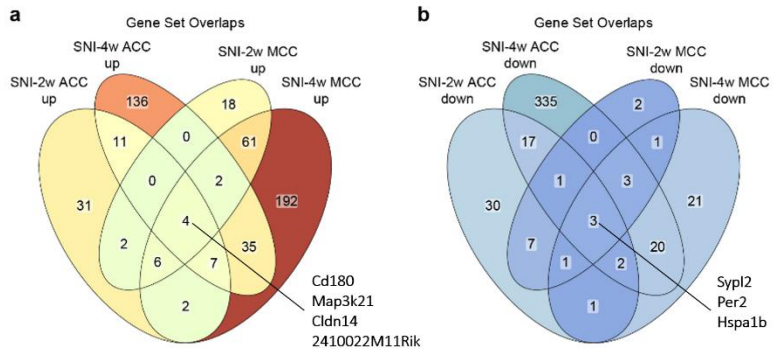

Figure 8. Integrated analysis of transcriptomic data. **a-b** Venn diagram depicting partial overlaps of up-regulated (a) and down-regulated (b) DEGs of SNI-2w (b) and SNI-4w (c) groups compared to sham group in cingulate subregions.

4. Discussion

Although molecular alterations within the cingulate cortex after NP have been explored in prior transcriptomic studies, these analyses have been largely restricted to single time points or confined to the ACC. Our study addresses this gap by systematically profiling temporal transcriptomic dynamics across two subregions of the cingulate cortex following prolonged peripheral nerve injury. We observed that the number of significantly enriched KEGG pathways increased over time within each cingulate subregion. Furthermore, the biological pathways enriched by DEGs were broadly conserved between the two major cingulate subdivisions. These data not only corroborate previously established roles for synaptic transmission/plasticity and neuroinflammation in NP but also reveal a novel pathogenic dimension: at the cortical level, NP shares fundamental pathophysiological mechanisms, such as proteostatic disruption and mitochondrial dysfunction, with neurodegenerative disorders.

Chronic pain is sustained in part by central sensitization—a form of synaptic plasticity characterized by heightened neuronal responsiveness within central nociceptive pathways following injury. At the cortical level, nociceptive inputs are transmitted via the thalamus to the ACC, enhancing synaptic plasticity and neuronal excitability in this region. LTP of glutamatergic transmission in the ACC represents a well-established model for studying the synaptic mechanisms underlying chronic pain [7]. Our transcriptomic profiling revealed an enrichment of DEGs in synaptic-related functions and pathways in the cingulate cortex of NP mice compared with sham controls, consistent with prior transcriptomic studies of the ACC [23–26]. We now proceed to summarize key advances in our understanding of these pathways in relation to cingulate synaptic mechanisms under NP conditions.

© 2026 by the author(s). Distributed under a Creative Commons CC BY license.

Preprints.org (www.preprints.org) | NOT PEER-REVIEWED | Posted: 27 April 2026 doi:10.20944/preprints202604.1802.v1

Peripheral nerve injury elicits excessive glutamate release, promoting Ca^{2+} influx into postsynaptic neurons through the activation of N-Methyl-D-Aspartate Receptors (NMDARs). The expression of NP-related cingulate LTP involves a multi-step signaling cascade dependent on Ca^{2+}-calmodulin (CaM). Central to this cascade, adenylyl cyclase 1 (AC1) converts ATP to cAMP, which in turn activates cAMP-dependent protein kinase A (PKA). PKA promotes the synthesis of diverse plasticity-related proteins via phosphorylation of the transcription factor cAMP response element-binding protein (CREB) in the nucleus [7,20]. In addition to cAMP signaling, activation of the MAPK pathway also contributes to CREB phosphorylation [78]. Collectively, these biochemical events enhance the phosphorylation and membrane trafficking of NMDARs and Ca^{2+}-permeable AMPAR, thereby amplifying postsynaptic responsiveness [7,20]. Furthermore, cAMP signaling is crucial for presynaptic LTP through downstream PKA-mediated signaling [79]. Correspondingly, selective pharmacological inhibition of the cAMP [80] or MAPK [81,82] pathway in the ACC attenuates behavioral hypersensitivity and associated negative affect in preclinical models of chronic pain, highlighting their potential as a therapeutic target for NP. Our data demonstrate an enrichment of ACC-derived DEGs in pathways central to synaptic modulation—including glutamatergic synapse, calcium, cAMP, and MAPK signaling—thereby lending mechanistic support to models of ACC synaptic dysregulation in chronic neuropathic pain.

In this study, KEGG pathway analysis highlighted the involvement of cholinergic synapse and oxytocin signaling pathways in the ACC under NP conditions. Cholinergic neuromodulation has been shown to mitigate NP by enhancing γ-Aminobutyric Acid Type A Receptor ($GABA_AR$)-mediated inhibitory transmission via muscarinic M1 receptors [83,84], while oxytocin alleviates chronic pain and associated emotional anxiety by restoring the balance between excitatory and inhibitory signaling in the ACC [85,86]. Notably, our analysis also revealed an enrichment of ECM-related DEGs in the cingulate cortex following NP induction. Beyond its classical structural role in providing cellular support, the ECM functions as a class of signaling molecules that act through adhesion receptors to dynamically regulate cellular responses to environmental perturbations, including noxious stimuli. Within the central nervous system (CNS), the ECM is recognized for its influence on synaptic plasticity and participation in diverse pathophysiological processes [87]. Supporting this, recent studies demonstrate that a key ECM component laminin-1 mediates the transduction of extracellular changes into intracellular synaptic remodeling in the ACC, thereby contributing to the development of NP and associated aversive affective states[75,76].

Central sensitization is further driven by neuroinflammation within both the peripheral and central nervous systems. A hallmark of neuroinflammation is the activation of glial cells—including microglia and astrocytes—in the spinal cord and brain, which promotes the release of proinflammatory cytokines and chemokines [88]. Under chronic pain conditions, astrocyte activation occurs in the ACC [89], leading to elevated levels of inflammatory cytokines such as TNF-α. TNF-α enhances synaptic transmission in the ACC via presynaptic mechanisms and also promotes necroptosis of parvalbumin-expressing interneurons, collectively shifting the excitatory–inhibitory (E/I) balance toward excitation [90,91]. Accordingly, intra-ACC administration of anti-TNF-α antibodies alleviates behavioural hypersensitivity and negative emotions associated with chronic pain [90,92,93]. Furthermore, NF-κB expression is markedly increased in the ACC under chronic pain conditions [94], and its selective inhibition attenuates pain-related hypersensitivity and affective disturbances [95]. Mechanistically, elevated TNF-α in the ACC activates the NF-κB pathway, up-regulating acid-sensing ion channel 1a and subsequently enhancing the activity of ACC glutamatergic neurons [95]. Additionally, the tripartite motif containing 14 (TRIM14)–NF-κB pathway in the ACC has been implicated in mediating chronic pain and its comorbid depression [92]. Previous transcriptomic studies have confirmed that DEGs in the ACC under chronic pain conditions are enriched in neuroinflammation-related pathways [24,27]. In line with these findings, our study reveals that DEGs in the cingulate cortex under neuropathic pain are enriched in the TNF and NF-κB signaling pathways, again underscoring the critical role of cortical neuroinflammatory mechanisms in the pathogenesis of chronic pain.

© 2026 by the author(s). Distributed under a Creative Commons CC BY license.

Preprints.org (www.preprints.org) | NOT PEER-REVIEWED | Posted: 27 April 2026 doi:10.20944/preprints202604.1802.v1

Beyond the well-established mechanisms of synaptic plasticity and neuroinflammation central to current research on ACC-mediated chronic pain, our functional analyses also reveal previously understudied regulatory pathways. Chronic pain shares potential mechanistic links with neurodegenerative diseases such as Alzheimer's disease and amyotrophic lateral sclerosis. Sustained pain can induce a persistent neuroinflammatory state, disrupt proteostasis [96], and cause mitochondrial dysfunction [97,98], processes analogous to those observed in neurodegeneration [99]. Having already addressed neuroinflammation in the cingulate cortex under NP conditions, we now focus on the latter two aspects. Autophagy, an evolutionarily conserved intracellular degradation system, delivers aged proteins and damaged organelles to lysosomes for breakdown. It plays a critical role in neuronal survival and synaptic homeostasis in the CNS [100]. Although autophagy is differentially regulated in spinal neurons and glial cells following peripheral nerve injury, dysregulated autophagic activity is recognized as a key contributor to the induction and maintenance of NP [101,102]. Generally, impaired autophagy exacerbates NP, whereas enhancing autophagic flux can attenuate pain-related behaviors, likely through modulation of inflammatory responses [101]. Accordingly, pharmacological agents that upregulate autophagy have shown promise in alleviating NP in preclinical models [103,104]. Recent evidence further indicates that autophagic dysfunction occurs in both neurons and microglia within the ACC under chronic pain conditions. This impairment promotes enhanced excitability of glutamatergic neurons via neuroinflammatory and synaptic plasticity pathways, thereby driving pain hypersensitivity and negative affect. Conversely, restoring autophagy in neural cells mitigates pain-related anxiety and hyperalgesia while reestablishing synaptic homeostasis [105–108]. Thus, cortical autophagy within the pain matrix represents a compelling direction for future investigation.

The "mitotoxicity hypothesis" of NP, first proposed in the context of chemotherapy-induced neuropathy, has subsequently been validated in models of peripheral nerve injury. These insults induce mitochondrial dysfunction in primary sensory neurons by disrupting key mitochondrial processes—including bioenergetics, transport, fusion, and mitophagy—and by elevating nitro-oxidative stress. Together, these alterations impair axonal growth and promote neuronal sensitization [109,110]. Mitophagy, the selective autophagic clearance of damaged mitochondria, represents a central mitochondrial quality-control mechanism. Its dysregulation in the peripheral nervous system leads to the accumulation of defective mitochondria, increased reactive oxygen species (ROS) generation, microglial activation, and myelin breakdown, thereby contributing to NP development [111,112]. At the SDH level, deficient mitophagy in microglia facilitates NOD-, LRR- and pyrin domain-containing protein 3 (NLRP3) inflammasome driven neuroinflammation via mitochondrial ROS, ultimately promoting pain-related plasticity in the CNS [113]. Accordingly, interventions that enhance mitophagy have demonstrated therapeutic efficacy in experimental NP models [109,113]. Notably, recent work has for the first time revealed that the PINK1/PARKIN dependent mitophagy pathway is impaired in the ACC of rats with NP. Treadmill exercise was shown to restore mitochondrial homeostasis by reactivating this pathway, leading to alleviation of pain-like behaviours [114]. These findings highlight mitochondrial dysfunction in the ACC as an important, yet still underexplored, component of NP pathophysiology that warrants further investigation.

Other pathways warranting discussion include the PI3K/Akt pathway and circadian rhythm regulation. PI3K exhibits dual enzymatic activity as both a protein kinase and a lipid kinase. Typically activated by cytokines and growth factors, it phosphorylates Akt, which subsequently orchestrates the activation or suppression of a broad spectrum of downstream effectors involved in cell survival, proliferation, and metabolism [115]. To our knowledge, only a single study has reported that inhibiting PI3K/Akt signalling in the ACC ameliorates both nociceptive responses and affective behaviors in a rodent model of cancer-induced pain [116], highlighting a significant gap in our understanding of its role in NP at cortical levels. The circadian modulation of NP is well-documented clinically [117]. Mechanistic investigations have largely focused on peripheral and spinal sites, along with descending pain modulatory systems [118]. In contrast, direct evidence for the involvement of

© 2026 by the author(s). Distributed under a Creative Commons CC BY license.

Preprints.org (www.preprints.org) | NOT PEER-REVIEWED | Posted: 27 April 2026 doi:10.20944/preprints202604.1802.v1

higher-order cortical and limbic structures in the circadian gating of pain perception remains notably scarce. Nevertheless, molecular oscillations with clear diurnal rhythms have been observed within these regions [119]. A growing body of transcriptomic studies has established significant dysregulation of core clock gene expression in the ACC under conditions of major depressive disorder [120]. Our own findings similarly point to an emerging relevance of circadian rhythm disruptions within the cingulate cortex in NP pathogenesis. Therefore, future studies are imperative to elucidate the precise mechanisms through which cortical and limbic circuits contribute to the circadian organization of pain processing.

Several limitations should be acknowledged in the present study. First, the cingulate cortex comprises heterogeneous cell populations, including distinct neuronal subtypes, astrocytes, and microglia. All bioinformatic analyses reported here were derived from bulk tissue, which integrates signals across these diverse cell types. Future work employing single-cell RNA or spatial transcriptomics will be essential to dissect cell type-specific transcriptional changes following NP. Second, while our study focused on transcriptional and pathway level alterations, it did not assess post-translational modifications—particularly rapid, phosphorylation dependent regulatory mechanisms known to modulate higher brain functions. Integrating multi-omics approaches, such as phosphoproteomics, metabolomics, and lipidomics, could reveal more refined molecular distinctions underlying NP. Third, although we identified transcriptomic changes and performed functional enrichment analyses in the cingulate cortex, whether these alterations causally contribute to the initiation or persistence of NP, and whether they represent viable therapeutic targets, remains to be experimentally validated. Further mechanistic and interventional studies are needed to establish their functional relevance and translational potential.

5. Conclusions

Collectively, these findings substantiate the involvement of synapse- and neuroinflammation-related mechanisms within the cingulate cortex in the pathophysiology of NP. Furthermore, they provide evidence suggesting that NP at the cortical level may share overlapping pathological mechanisms with neurodegenerative disorders. Our data contribute to a deeper understanding of NP etiology and offer a theoretical foundation for developing novel therapeutic strategies.

Author Contributions: Conceptualization, Y.B., F.F., and Y.G.D.; methodology, X.T.Q.; software, G.Q.Y. and Z.R.Y.; validation, G.Q.Y., C.G.J. and C.Z.; formal analysis, G.Q.Y.; investigation, G.X.P.; resources, H.M.; data curation, X.T.Q.; writing—original draft preparation, Y.B.; writing—review and editing, Y.B., F.F., and Y.G.D.; visualization, Y.B.; supervision, Z.H.Z.; project administration, X.T.Q. and G.Q.Y.; funding acquisition, Y.B. and G.Q.Y. All authors have read and agreed to the published version of the manuscript. G.Q.Y., Z.R.Y., and X.T.Q. contributed equally to this work.

Funding: This research was supported by National Natural Science Foundation of China (No. 82101318 to Y.B.), Liaoning Provincial Joint Science and Technology Program (No. 2025-MSLH-731 to G.Q.Y. and No. 2023-MSLH-345 to Y.B.), and the Research Project of General Hospital of Northern Theater Command (No. ZZKY2024067 to G.Q.Y.).

Institutional Review Board Statement: The animal study protocol was approved by the Institutional Review Board of the General Hospital of Northern Theater Command (protocol code Y-2025-105).

Data Availability Statement: All raw sequence data have been deposited in the NCBI Sequence Read Archive under the accession number PRJNA1401302 (available at: https://dataview.ncbi.nlm.nih.gov/object/PRJNA1401302).

Acknowledgments: We are grateful to Amy Qin (Shanghai Glossop Biotech Co. ltd) for her help with the illustrations.

Conflicts of Interest: The authors declare no conflicts of interest.

© 2026 by the author(s). Distributed under a Creative Commons CC BY license.

Preprints.org (www.preprints.org) | NOT PEER-REVIEWED | Posted: 27 April 2026 doi:10.20944/preprints202604.1802.v1

Abbreviations

The following abbreviations are used in this manuscript:

ACC	Anterior Cingulate Cortex
AC1	Adenylyl Cyclase 1
CaM	Calmodulin
cAMP	Cyclic Adenosine Monophosphate
CNS	Central Nervous System
CREB	cAMP Response Element-Binding Protein
DEGs	Differentially Expressed Genes
ECM	Extracellular Matrix
E/I	Excitatory–Inhibitory
GO	Gene Ontology
GPCRs	G Protein-Coupled Receptors
KEGG	Kyoto Encyclopedia of Genes and Genomes
LTP	Long-Term Potentiation
MAPK	Mitogen-Activated Protein Kinase
MCC	Midcingulate Cortex
MEs	Module Eigengenes
MWTs	Mechanical Withdrawal Thresholds
NF-κB	Nuclear Factor Kappa B
NLRP3	NOD-, LRR- and Pyrin Domain-Containing Protein 3
NMDAR	N-Methyl-D-Aspartate Receptor
NP	Neuropathic Pain
PI3K-Akt	Phosphoinositide 3-Kinase–Protein Kinase B
PKA	Protein Kinase A
PPI	Protein-Protein Interaction
ROS	Reactive Oxygen Species
SDH	Spinal Dorsal Horn
SNI	Spared Nerve Injury
TFs	Transcription Factors
TGF-β	Transforming Growth Factor-Beta
TNF	Tumor Necrosis Factor
TRIM14	Tripartite Motif Containing 14
WGCNA	Weighted Gene Co-expression Network Analysis

Appendix A

© 2026 by the author(s). Distributed under a Creative Commons CC BY license.

Preprints.org (www.preprints.org) | NOT PEER-REVIEWED | Posted: 27 April 2026 doi:10.20944/preprints202604.1802.v1

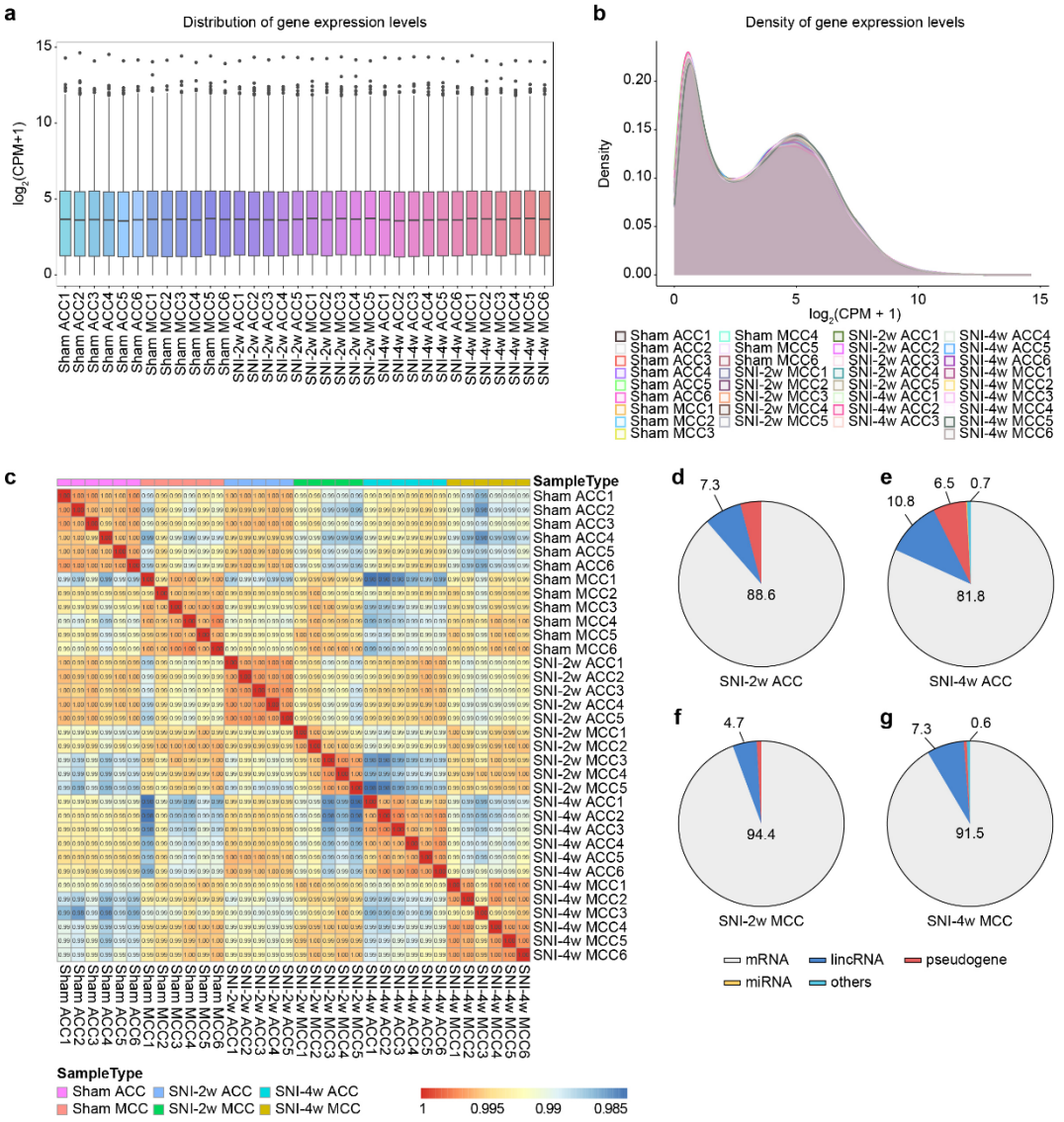

Figure A1. The quality of RNA-seq data from each sample. **a** Boxplot showing the distribution of gene expression levels in each cingulate cortex sample. **b** Distribution diagram showing the density of gene expression levels in each cingulate cortex sample. **c** Pearson correlation analysis results. **d** The constituent ratio of the identified DEGs.

© 2026 by the author(s). Distributed under a Creative Commons CC BY license.

Preprints.org (www.preprints.org) | NOT PEER-REVIEWED | Posted: 27 April 2026 doi:10.20944/preprints202604.1802.v1

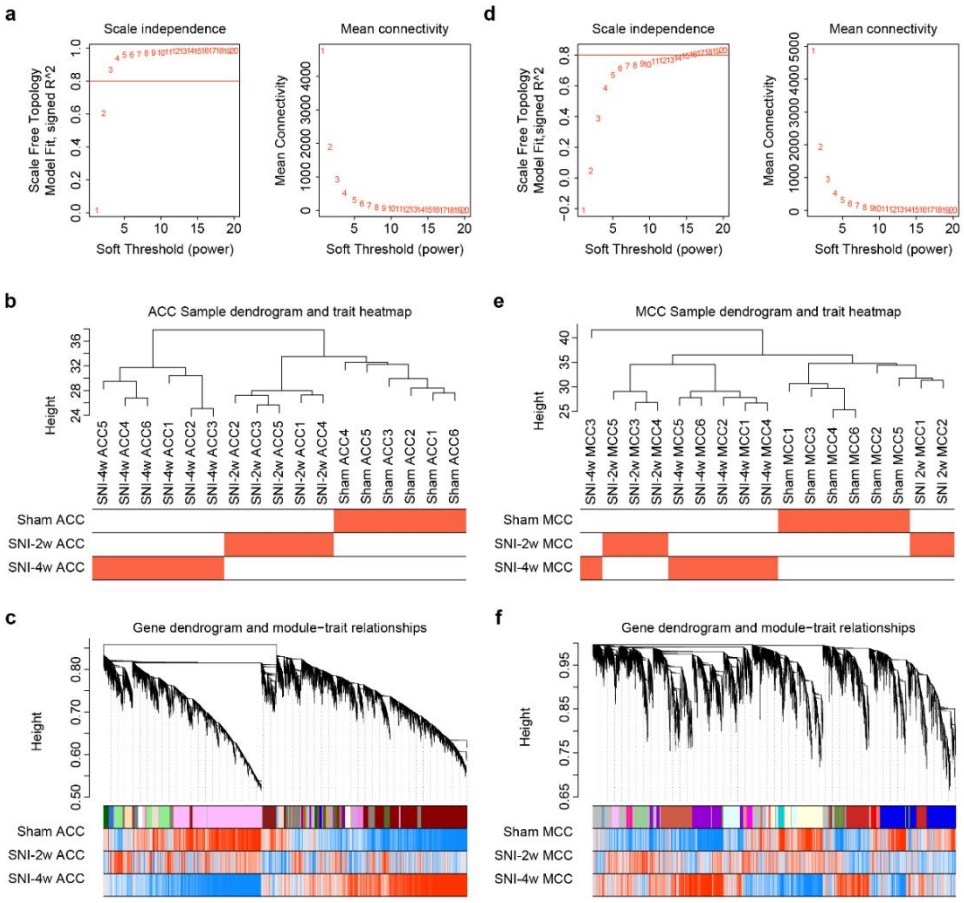

Figure A2. Construction of WGCNA network. **a** Weighting coefficient β selection in the ACC. The left panel displays the scale-free topology model fit index (R^2) across a range of soft-thresholding powers, while the right panel shows the corresponding average connectivity. Connectivity distribution of nodes with β set as 3 (left panel) and the verification of scale-free topology with β set as 3 (right panel). **b** Modules were clustered, and correlations were investigated with a sample dendrogram. **c** Gene clustering dendrogram and module detection. The dendrogram illustrates hierarchical clustering of genes, with distinct modules identified using the dynamic tree-cutting method and indicated by assigned colors. **d-f** Construction of WGCNA network in the MCC. Connectivity distribution of nodes with β set as 14 (left panel in d) and the verification of scale-free topology with β set as 14 (right panel in d). The conventions are the same as those in a-c.

Table A1. The summary of raw general RNA-sequencing data set in RNA sequencing.

Sample	Raw data read	Valid data read	Valid ratio%	Mapped rate%	Q20%	Q30%
Sham ACC1	21818051	21643187	99.20	98.70	99.03	95.66
Sham ACC2	21587870	21420444	99.22	98.70	98.99	95.40
Sham ACC3	21569341	21398228	99.21	98.80	99.02	95.53
Sham ACC4	21947667	21775563	99.22	98.80	99.01	95.50
Sham ACC5	21869294	21700825	99.23	98.70	99.01	95.49
Sham ACC6	22152128	21975089	99.20	98.80	99.01	95.52
SNI-2w ACC1	22308621	22121100	99.16	98.80	99.00	95.48
SNI-2w ACC2	23851517	23652719	99.17	98.80	98.96	95.27
SNI-2w ACC3	26272018	26032632	99.09	98.80	98.97	95.33
SNI-2w ACC4	26117787	25882816	99.10	98.80	98.93	95.17
SNI-2w ACC5	25422486	25222963	99.22	98.70	98.99	95.41
SNI-4w ACC1	24424491	24231291	99.21	98.70	98.95	95.28

© 2026 by the author(s). Distributed under a Creative Commons CC BY license.

Preprints.org (www.preprints.org) | NOT PEER-REVIEWED | Posted: 27 April 2026 doi:10.20944/preprints202604.1802.v1

SNI-4w ACC2	26116098	25886414	99.12	98.50	98.94	95.24
SNI-4w ACC3	24611453	24409985	99.18	98.70	98.96	95.28
SNI-4w ACC4	23637283	23454763	99.23	98.80	98.94	95.15
SNI-4w ACC5	25872247	25683668	99.27	98.80	99.00	95.42
SNI-4w ACC6	25735743	25524141	99.18	98.80	99.00	95.48
Sham MCC1	28310668	28075670	99.17	98.70	98.98	95.37
Sham MCC2	26206389	25981769	99.14	98.70	98.99	95.41
Sham MCC3	24960891	24764247	99.21	98.60	98.96	95.25
Sham MCC4	24349730	24140681	99.14	98.60	98.97	95.33
Sham MCC5	24049610	23868263	99.25	99.00	99.08	95.79
SNI-2w MCC1	26830426	26639099	99.29	98.90	99.06	95.67
SNI-2w MCC2	25049360	24860351	99.25	98.90	99.03	95.54
SNI-2w MCC3	25136432	24939615	99.22	98.80	98.97	95.35
SNI-2w MCC4	24317017	24159519	99.35	98.90	99.07	95.67
SNI-2w MCC5	25713271	25505292	99.19	98.80	98.94	95.21
SNI-2w MCC6	24828567	24621943	99.17	98.80	99.00	95.42
SNI-4w MCC1	27693727	27465768	99.18	98.70	98.94	95.20
SNI-4w MCC2	26213380	26003592	99.20	98.8	98.97	95.29
SNI-4w MCC3	25283618	25087761	99.23	98.70	98.99	95.42
SNI-4w MCC4	29172720	28923281	99.14	98.70	98.97	95.37
SNI-4w MCC5	21818051	21643187	99.20	98.70	99.03	95.66
SNI-4w MCC6	21587870	21420444	99.22	98.70	98.99	95.40

Table A2. A reference set of genes encoding synapse-related molecules, G protein-coupled receptors, ion channels, and neuropeptides.

Types	Genes
Synapse-related molecules	Agt Cadps2 Chat Cplx1 Napb Slc17a7 Slc18a3 Slc5a7 Snca Sncg Stxbp5l Sv2b Syt6 Syt9 Ywhaz Abat Atp2a2 Atp2b2 Baiap3 Cadps Camk2a Cd47 Clu Lin7a Nat8l Nlgn1 Nrxn3 Ntrk2 Pak1 Pde1b Rph3a Sirpa Slc17a6 Slc1a2 Slc6a1 Slc6a7 Sv2a Syn2 Syp Syt11 Vamp1 Ryr2 Ryr3 Itpr1 Itpr2 Itpr3 Nlgn1 Pde4b Calm1
Ion channels	Ano1 Cacnb3 Cacng5 Chrna3 Chrna4 Chrnb3 Chrnb4 Kcna2 Kcnd2 Kcng4 Kcnip1 Kcnip3 Kcnma1 Kcnmb4 Lrrc55 Cacna1b Cacna1g Cacna1i Cacna2d1 Cacng2 Gabrb1 Gabrg2 Gabrg3 Glrb Hcn2 Kcna6 Kcnab2 Kcnc1 Kcnc2 Kcnc4 Kcnip4 Kcnj3 Scn1a Scn1b Ttyh1 Gabra1 Gabra2 Gabra3 Gabra4 Gabra5 Gabrb1 Gabrb2 Gabrb3 Gria1 Gria2 Gria3 Gria4 Grid1 Grid2 Grik1 Grik2 Grik3 Grik4 Grik5 Grin1 Grin2a Grin2b Grin2c Grin3a P2rx1 P2rx4 P2rx7
G protein-coupled receptors	Ackr1 Ackr3 Adcyap1r1 Adgra1 Adgra2 Adgra3 Adgrb1 Adgrb2 Adgrb3 Adgrd1 Adgre1 Adgre5 Adgrf4 Adgrf5 Adgrg1 Adgrg2 Adgrg3 Adgrg6 Adgrl1 Adgrl2 Adgrl3 Adgrl4 Adgrv1 Adora1 Adora2b Adora3 Adra1a Adra1b Adra2a Adra2b Adra2c Adrb1 Adrb2 Adrb3 Agtr2 Agtrap ApInr Avpr1a C3ar1 C5ar1 C5ar2 Calcrl Cckbr Ccr1 Ccr10 Ccr5 Ccr7 Ccrl2 Celsr1 Celsr2 Celsr3 Chrm1 Chrm2 Chrm3 Chrm5 Cmklr1 Cnr1 Crcp Crhr1 Crhr2 Cx3cr1 Cxcr2 Cxcr4 Cysltr1 Drd1 Drd4 Drd5 Ednra Ednrb F2r F2rl3 Ffar1 Fpr2 Fzd1 Fzd10 Fzd2 Fzd3 Fzd4 Fzd5 Fzd6 Fzd7 Fzd8 Fzd9 Gabbr1 Gabbr2 Galr1 Ghsr Gipr Gper1 Gpr1 Gpr101 Gpr12 Gpr135 Gpr139 Gpr141 Gpr149 Gpr150 Gpr151 Gpr152 Gpr153 Gpr156 Gpr157 Gpr158 Gpr160 Gpr161 Gpr162 Gpr17 Gpr173 Gpr176 Gpr182 Gpr19 Gpr21 Gpr22 Gpr26 Gpr27 Gpr3 Gpr34 Gpr35 Gpr37 Gpr37l1 Gpr4 Gpr45 Gpr50 Gpr55 Gpr6 Gpr61 Gpr62 Gpr68 Gpr75 Gpr83 Gpr85 Gpr88 Gprc5b Gprc5c Grm1 Grm2 Grm3 Grm4 Grm5 Grm7 Grm8 Grpr Hcrtr1 Hcrtr2 Hrh1 Hrh2 Hrh3 Htr1a Htr1b Htr1d Htr1f Htr2a Htr2c Htr4 Htr5a Htr5b Htr6 Htr7 Kiss1r Lgr4 Lgr5 Lgr6 Lpar1 Lpar4 Lpar6 Ltb4r1 Mc1r Mc3r Mc4r Mchr1 Mtnr1a Nmbr Nmur2 Npbwr1

© 2026 by the author(s). Distributed under a Creative Commons CC BY license.

Preprints.org (www.preprints.org) | NOT PEER-REVIEWED | Posted: 27 April 2026 doi:10.20944/preprints202604.1802.v1

	Npr3 Npy1r Npy2r Npy5r Ntsr1 Ntsr2 Ogfr Ogfrl1 Oprk1 Oprl1 Oprm1 Oxgr1 Oxtr P2ry1 P2ry12 P2ry13 P2ry14 P2ry2 P2ry6 Pgr15l Ppard Prokr2 Ptgdr Ptger1 Ptger2 Ptger3 Ptger4 Ptgfr Ptgir Pth1r Ramp1 Ramp2 Ramp3 Rorb Rxfp1 Rxfp2 Rxfp3 S1pr1 S1pr2 S1pr3 S1pr5 Sigmar1 Smo Sstr1 Sstr2 Sstr3 Sstr4 Sstr5 Sucnr1 Tacr1 Tacr3 Tas1r1 Tas1r3 Tbxa2r Trhr Trhr2 Uts2r Vipr1 Vipr2 Vmn1r4 Vmn2r29 Vmn2r84 Vmn2r87 Xcr1
Neuropeptides	Adcyap1 Agrp Calca Cartpt Cort Gal Grp Hcrt Nmb Nms Npb Npff Nppa Nps Npy Pcsk1n Pdyn Penk Pnoc Pomc Prok2 Pth2 Qrfp Scg5 Tac1 Tac2 Ecel1 Tenm1 Tyro3 Rapgef2 Sort1

References

1. Finnerup, N. B.; Kuner, R.; Jensen, T. S., Neuropathic Pain: From Mechanisms to Treatment. *Physiological reviews* **2021,** 101, (1), 259-301.
2. Scholz, J.; Finnerup, N. B.; Attal, N.; Aziz, Q.; Baron, R.; Bennett, M. I.; Benoliel, R.; Cohen, M.; Cruccu, G.; Davis, K. D.; Evers, S.; First, M.; Giamberardino, M. A.; Hansson, P.; Kaasa, S.; Korwisi, B.; Kosek, E.; Lavand'homme, P.; Nicholas, M.; Nurmikko, T.; Perrot, S.; Raja, S. N.; Rice, A. S. C.; Rowbotham, M. C.; Schug, S.; Simpson, D. M.; Smith, B. H.; Svensson, P.; Vlaeyen, J. W. S.; Wang, S. J.; Barke, A.; Rief, W.; Treede, R. D., The IASP classification of chronic pain for ICD-11: chronic neuropathic pain. *Pain* **2019,** 160, (1), 53-59.
3. Cohen, S. P.; Vase, L.; Hooten, W. M., Chronic pain: an update on burden, best practices, and new advances. *Lancet (London, England)* **2021,** 397, (10289), 2082-2097.
4. Gomez-Varela, D.; Barry, A. M.; Schmidt, M., Proteome-based systems biology in chronic pain. *Journal of proteomics* **2019,** 190, 1-11.
5. Starobova, H.; S, W. A. H.; Lewis, R. J.; Vetter, I., Transcriptomics in pain research: insights from new and old technologies. *Molecular omics* **2018,** 14, (6), 389-404.
6. Vogt, B. A., Pain and emotion interactions in subregions of the cingulate gyrus. *Nat Rev Neurosci* **2005,** 6, (7), 533-44.
7. Bliss, T. V.; Collingridge, G. L.; Kaang, B. K.; Zhuo, M., Synaptic plasticity in the anterior cingulate cortex in acute and chronic pain. *Nature reviews. Neuroscience* **2016,** 17, (8), 485-96.
8. Lee, D. E.; Kim, S. J.; Zhuo, M., Comparison of behavioral responses to noxious cold and heat in mice. *Brain research* **1999,** 845, (1), 117-21.
9. Zhuo, M., Molecular mechanisms of pain in the anterior cingulate cortex. *Journal of neuroscience research* **2006,** 84, (5), 927-33.
10. Johansen, J. P.; Fields, H. L.; Manning, B. H., The affective component of pain in rodents: direct evidence for a contribution of the anterior cingulate cortex. *Proceedings of the National Academy of Sciences of the United States of America* **2001,** 98, (14), 8077-82.
11. Tang, J.; Ko, S.; Ding, H. K.; Qiu, C. S.; Calejesan, A. A.; Zhuo, M., Pavlovian fear memory induced by activation in the anterior cingulate cortex. *Molecular pain* **2005,** 1, 6.
12. Delevich, K.; Tucciarone, J.; Huang, Z. J.; Li, B., The mediodorsal thalamus drives feedforward inhibition in the anterior cingulate cortex via parvalbumin interneurons. *The Journal of neuroscience : the official journal of the Society for Neuroscience* **2015,** 35, (14), 5743-53.
13. Kang, S. J.; Kwak, C.; Lee, J.; Sim, S. E.; Shim, J.; Choi, T.; Collingridge, G. L.; Zhuo, M.; Kaang, B. K., Bidirectional modulation of hyperalgesia via the specific control of excitatory and inhibitory neuronal activity in the ACC. *Molecular brain* **2015,** 8, (1), 81.
14. Zhu, X.; Tang, H. D.; Dong, W. Y.; Kang, F.; Liu, A.; Mao, Y.; Xie, W.; Zhang, X.; Cao, P.; Zhou, W.; Wang, H.; Farzinpour, Z.; Tao, W.; Song, X.; Zhang, Y.; Xue, T.; Jin, Y.; Li, J.; Zhang, Z., Distinct thalamocortical circuits underlie allodynia induced by tissue injury and by depression-like states. *Nature neuroscience* **2021,** 24, (4), 542-553.
15. Meda, K. S.; Patel, T.; Braz, J. M.; Malik, R.; Turner, M. L.; Seifikar, H.; Basbaum, A. I.; Sohal, V. S., Microcircuit Mechanisms through which Mediodorsal Thalamic Input to Anterior Cingulate Cortex Exacerbates Pain-Related Aversion. *Neuron* **2019,** 102, (5), 944-959.e3.

© 2026 by the author(s). Distributed under a Creative Commons CC BY license.

Preprints.org (www.preprints.org) | NOT PEER-REVIEWED | Posted: 27 April 2026 doi:10.20944/preprints202604.1802.v1

16. Chen, T.; Taniguchi, W.; Chen, Q. Y.; Tozaki-Saitoh, H.; Song, Q.; Liu, R. H.; Koga, K.; Matsuda, T.; Kaito-Sugimura, Y.; Wang, J.; Li, Z. H.; Lu, Y. C.; Inoue, K.; Tsuda, M.; Li, Y. Q.; Nakatsuka, T.; Zhuo, M., Top-down descending facilitation of spinal sensory excitatory transmission from the anterior cingulate cortex. *Nat Commun* **2018,** 9, (1), 1886.
17. Zhuang, X.; Huang, L.; Gu, Y.; Wang, L.; Zhang, R.; Zhang, M.; Li, F.; Shi, Y.; Mo, Y.; Dai, Q.; Wei, C.; Wang, J., The anterior cingulate cortex projection to the dorsomedial striatum modulates hyperalgesia in a chronic constriction injury mouse model. *Archives of medical science : AMS* **2021,** 17, (5), 1388-1399.
18. Gao, S. H.; Shen, L. L.; Wen, H. Z.; Zhao, Y. D.; Chen, P. H.; Ruan, H. Z., The projections from the anterior cingulate cortex to the nucleus accumbens and ventral tegmental area contribute to neuropathic pain-evoked aversion in rats. *Neurobiology of disease* **2020,** 140, 104862.
19. Zhuo, M., Cortical excitation and chronic pain. *Trends in neurosciences* **2008,** 31, (4), 199-207.
20. Xu, H.; Wu, L. J.; Wang, H.; Zhang, X.; Vadakkan, K. I.; Kim, S. S.; Steenland, H. W.; Zhuo, M., Presynaptic and postsynaptic amplifications of neuropathic pain in the anterior cingulate cortex. *The Journal of neuroscience : the official journal of the Society for Neuroscience* **2008,** 28, (29), 7445-53.
21. Wang, H.; Xu, H.; Wu, L. J.; Kim, S. S.; Chen, T.; Koga, K.; Descalzi, G.; Gong, B.; Vadakkan, K. I.; Zhang, X.; Kaang, B. K.; Zhuo, M., Identification of an adenylyl cyclase inhibitor for treating neuropathic and inflammatory pain. *Science translational medicine* **2011,** 3, (65), 65ra3.
22. Li, X. Y.; Ko, H. G.; Chen, T.; Descalzi, G.; Koga, K.; Wang, H.; Kim, S. S.; Shang, Y.; Kwak, C.; Park, S. W.; Shim, J.; Lee, K.; Collingridge, G. L.; Kaang, B. K.; Zhuo, M., Alleviating neuropathic pain hypersensitivity by inhibiting PKMzeta in the anterior cingulate cortex. *Science (New York, N.Y.)* **2010,** 330, (6009), 1400-4.
23. Dai, W.; Huang, S.; Luo, Y.; Cheng, X.; Xia, P.; Yang, M.; Zhao, P.; Zhang, Y.; Lin, W. J.; Ye, X., Sex-Specific Transcriptomic Signatures in Brain Regions Critical for Neuropathic Pain-Induced Depression. *Frontiers in molecular neuroscience* **2022,** 15, 886916.
24. Kang, X.; Si, J.; Zhang, J.; Yan, X.; Yu, Z.; Zhang, Y.; Li, X.; Wu, L. A., Combined Transcriptomic and Proteomic Profiling of the Mouse Anterior Cingulate Cortex Identifies Potential Therapeutic Targets for Pulpitis-Induced Pain. *ACS Omega* **2024,** 9, (5), 5972-5984.
25. Qiu, X. T.; Guo, C.; Ma, L. T.; Li, X. N.; Zhang, Q. Y.; Huang, F. S.; Zhang, M. M.; Bai, Y.; Liang, G. B.; Li, Y. Q., Transcriptomic and proteomic profiling of the anterior cingulate cortex in neuropathic pain model rats. *Frontiers in molecular neuroscience* **2023,** 16, 1164426.
26. Su, S.; Li, M.; Wu, D.; Cao, J.; Ren, X.; Tao, Y. X.; Zang, W., Gene Transcript Alterations in the Spinal Cord, Anterior Cingulate Cortex, and Amygdala in Mice Following Peripheral Nerve Injury. *Frontiers in cell and developmental biology* **2021,** 9, 634810.
27. Zhang, Y.; Jiang, S.; Liao, F.; Huang, Z.; Yang, X.; Zou, Y.; He, X.; Guo, Q.; Huang, C., A transcriptomic analysis of neuropathic pain in the anterior cingulate cortex after nerve injury. *Bioengineered* **2022,** 13, (2), 2058-2075.
28. Vogt, B. A., Midcingulate cortex: Structure, connections, homologies, functions and diseases. *J Chem Neuroanat* **2016,** 74, 28-46.
29. Kragel, P. A.; Kano, M.; Van Oudenhove, L.; Ly, H. G.; Dupont, P.; Rubio, A.; Delon-Martin, C.; Bonaz, B. L.; Manuck, S. B.; Gianaros, P. J.; Ceko, M.; Reynolds Losin, E. A.; Woo, C. W.; Nichols, T. E.; Wager, T. D., Generalizable representations of pain, cognitive control, and negative emotion in medial frontal cortex. *Nature neuroscience* **2018,** 21, (2), 283-289.
30. Glass, J. M.; Williams, D. A.; Fernandez-Sanchez, M. L.; Kairys, A.; Barjola, P.; Heitzeg, M. M.; Clauw, D. J.; Schmidt-Wilcke, T., Executive function in chronic pain patients and healthy controls: different cortical activation during response inhibition in fibromyalgia. *J Pain* **2011,** 12, (12), 1219-29.
31. Fallon, N.; Chiu, Y.; Nurmikko, T.; Stancak, A., Functional Connectivity with the Default Mode Network Is Altered in Fibromyalgia Patients. *PloS one* **2016,** 11, (7), e0159198.
32. Blankstein, U.; Chen, J.; Diamant, N. E.; Davis, K. D., Altered brain structure in irritable bowel syndrome: potential contributions of pre-existing and disease-driven factors. *Gastroenterology* **2010,** 138, (5), 1783-9.
33. Li, X.; Zhu, Y.; Sun, H.; Shen, Z.; Sun, J.; Xiao, S.; He, X.; Liu, B.; Wang, Y.; Hu, Y.; Liu, B.; Liang, Y.; Jiang, Y.; Du, J.; Xu, C.; Fang, J.; Shao, X., Electroacupuncture Inhibits Pain Memory and Related Anxiety-Like

© 2026 by the author(s). Distributed under a Creative Commons CC BY license.

Preprints.org (www.preprints.org) | NOT PEER-REVIEWED | Posted: 27 April 2026 doi:10.20944/preprints202604.1802.v1

Behaviors by Blockading the GABA(B) Receptor Function in the Midcingulate Cortex. *Molecular neurobiology* **2023,** 60, (11), 6613-6626.

34. Kisler, L. B.; Granovsky, Y.; Sinai, A.; Sprecher, E.; Shamay-Tsoory, S.; Weissman-Fogel, I., Sex dimorphism in a mediatory role of the posterior midcingulate cortex in the association between anxiety and pain sensitivity. *Exp Brain Res* **2016,** 234, (11), 3119-3131.
35. Hong, J.; Li, J. N.; Wu, F. L.; Bao, S. Y.; Sun, H. X.; Zhu, K. H.; Cai, Z. P.; Li, F.; Li, Y. Q., Projections from anteromedial thalamus nucleus to the midcingulate cortex mediate pain and anxiety-like behaviors in mice. *Neurochem Int* **2023,** 171, 105640.
36. Hu, T. T.; Wang, R. R.; Du, Y.; Guo, F.; Wu, Y. X.; Wang, Y.; Wang, S.; Li, X. Y.; Zhang, S. H.; Chen, Z., Activation of the Intrinsic Pain Inhibitory Circuit from the Midcingulate Cg2 to Zona Incerta Alleviates Neuropathic Pain. *The Journal of neuroscience : the official journal of the Society for Neuroscience* **2019,** 39, (46), 9130-9144.
37. Tan, L. L.; Pelzer, P.; Heinl, C.; Tang, W.; Gangadharan, V.; Flor, H.; Sprengel, R.; Kuner, T.; Kuner, R., A pathway from midcingulate cortex to posterior insula gates nociceptive hypersensitivity. *Nature neuroscience* **2017,** 20, (11), 1591-1601.
38. Bortsov, A.; Esfahani, S. J.; Lima, L. V.; Ji, R. R.; Mogil, J. S.; Diatchenko, L., How people resolve pain: insights from human transcriptomics into immune activation and therapeutic innovations. *Pain* **2025,** 166, (11s), S60-s64.
39. Nie, L.; Wu, G.; Culley, D. E.; Scholten, J. C.; Zhang, W., Integrative analysis of transcriptomic and proteomic data: challenges, solutions and applications. *Critical reviews in biotechnology* **2007,** 27, (2), 63-75.
40. Ma, L. T.; Bai, Y.; Cao, P.; Ren, K. X.; Chen, J.; Zhang, T.; Fan, B. Y.; Qiao, Y.; Yan, H. Y.; Wang, J. J.; Li, Y. Q.; Zheng, J., The analgesic effects of β-elemene in rats with neuropathic pain by inhibition of spinal astrocytic ERK activation. *Molecular pain* **2022,** 18, 17448069221121562.
41. Ong, W. Y.; Stohler, C. S.; Herr, D. R., Role of the Prefrontal Cortex in Pain Processing. *Molecular neurobiology* **2019,** 56, (2), 1137-1166.
42. Bai, Y.; Ma, L. T.; Chen, Y. B.; Ren, D.; Chen, Y. B.; Li, Y. Q.; Sun, H. K.; Qiu, X. T.; Zhang, T.; Zhang, M. M.; Yi, X. N.; Chen, T.; Li, H.; Fan, B. Y.; Li, Y. Q., Anterior insular cortex mediates hyperalgesia induced by chronic pancreatitis in rats. *Molecular brain* **2019,** 12, (1), 76.
43. Ren, D.; Li, J. N.; Qiu, X. T.; Wan, F. P.; Wu, Z. Y.; Fan, B. Y.; Zhang, M. M.; Chen, T.; Li, H.; Bai, Y.; Li, Y. Q., Anterior Cingulate Cortex Mediates Hyperalgesia and Anxiety Induced by Chronic Pancreatitis in Rats. *Neuroscience bulletin* **2022,** 38, (4), 342-358.
44. Langfelder, P.; Horvath, S., WGCNA: an R package for weighted correlation network analysis. *BMC Bioinformatics* **2008,** 9, 559.
45. Szklarczyk, D.; Gable, A. L.; Lyon, D.; Junge, A.; Wyder, S.; Huerta-Cepas, J.; Simonovic, M.; Doncheva, N. T.; Morris, J. H.; Bork, P.; Jensen, L. J.; Mering, C. V., STRING v11: protein-protein association networks with increased coverage, supporting functional discovery in genome-wide experimental datasets. *Nucleic acids research* **2019,** 47, (D1), D607-d613.
46. Campbell, A. P.; Smrcka, A. V., Targeting G protein-coupled receptor signalling by blocking G proteins. *Nature reviews. Drug discovery* **2018,** 17, (11), 789-803.
47. Bouali-Benazzouz, R.; Landry, M.; Benazzouz, A.; Fossat, P., Neuropathic pain modeling: Focus on synaptic and ion channel mechanisms. *Progress in neurobiology* **2021,** 201, 102030.
48. Neugebauer, V.; Mazzitelli, M.; Cragg, B.; Ji, G.; Navratilova, E.; Porreca, F., Amygdala, neuropeptides, and chronic pain-related affective behaviors. *Neuropharmacology* **2020,** 170, 108052.
49. Hashikawa, Y.; Hashikawa, K.; Rossi, M. A.; Basiri, M. L.; Liu, Y.; Johnston, N. L.; Ahmad, O. R.; Stuber, G. D., Transcriptional and Spatial Resolution of Cell Types in the Mammalian Habenula. *Neuron* **2020,** 106, (5), 743-758.e5.
50. Wang, J. H.; Wu, C.; Lian, Y. N.; Cao, X. W.; Wang, Z. Y.; Dong, J. J.; Wu, Q.; Liu, L.; Sun, L.; Chen, W.; Chen, W. J.; Zhang, Z.; Zhuo, M.; Li, X. Y., Single-cell RNA sequencing uncovers the cell type-dependent transcriptomic changes in the retrosplenial cortex after peripheral nerve injury. *Cell reports* **2023,** 42, (12), 113551.

© 2026 by the author(s). Distributed under a Creative Commons CC BY license.

Preprints.org (www.preprints.org) | NOT PEER-REVIEWED | Posted: 27 April 2026 doi:10.20944/preprints202604.1802.v1

51. Brumovsky, P.; Shi, T. S.; Landry, M.; Villar, M. J.; Hökfelt, T., Neuropeptide tyrosine and pain. *Trends Pharmacol Sci* **2007,** 28, (2), 93-102.
52. Nelson, T. S.; Allen, H. N.; Khanna, R., Neuropeptide Y and Pain: Insights from Brain Research. *ACS Pharmacol Transl Sci* **2024,** 7, (12), 3718-3728.
53. Wang, W.; Yuan, M.; Xu, Y.; Yang, J.; Wang, X.; Zhou, Y.; Yu, Z.; Lu, Z.; Wang, Y.; Hu, C.; Bai, Q.; Li, Z., Prokineticin-2 Participates in Chronic Constriction Injury-Triggered Neuropathic Pain and Anxiety via Regulated by NF-κB in Nucleus Accumbens Shell in Rats. *Molecular neurobiology* **2024,** 61, (5), 2764-2783.
54. Li, Z. X.; Liu, B. W.; He, Z. G.; Xiang, H. B., Melanocortin-4 receptor regulation of pain. *Biochim Biophys Acta Mol Basis Dis* **2017,** 1863, (10 Pt A), 2515-2522.
55. Hain, H. S.; Belknap, J. K.; Mogil, J. S., Pharmacogenetic evidence for the involvement of 5-hydroxytryptamine (Serotonin)-1B receptors in the mediation of morphine antinociceptive sensitivity. *J Pharmacol Exp Ther* **1999,** 291, (2), 444-9.
56. Zhang, Y.; Xiao, X.; Zhang, X. M.; Zhao, Z. Q.; Zhang, Y. Q., Estrogen facilitates spinal cord synaptic transmission via membrane-bound estrogen receptors: implications for pain hypersensitivity. *The Journal of biological chemistry* **2012,** 287, (40), 33268-81.
57. Chen, S.; Kadakia, F.; Davidson, S., Group II metabotropic glutamate receptor expressing neurons in anterior cingulate cortex become sensitized after inflammatory and neuropathic pain. *Molecular pain* **2020,** 16, 1744806920915339.
58. Kim, H.; Kim, J.; Lee, H.; Shin, E.; Kang, H.; Jeon, J.; Youn, B., Baiap3 regulates depressive behaviors in mice via attenuating dense core vesicle trafficking in subsets of prefrontal cortex neurons. *Neurobiol Stress* **2022,** 16, 100423.
59. Pol, O., The role of carbon monoxide, heme oxygenase 1, and the Nrf2 transcription factor in the modulation of chronic pain and their interactions with opioids and cannabinoids. *Med Res Rev* **2021,** 41, (1), 136-155.
60. Masuda, T.; Iwamoto, S.; Yoshinaga, R.; Tozaki-Saitoh, H.; Nishiyama, A.; Mak, T. W.; Tamura, T.; Tsuda, M.; Inoue, K., Transcription factor IRF5 drives P2X4R+-reactive microglia gating neuropathic pain. *Nat Commun* **2014,** 5, 3771.
61. Zhang, F.; Gigout, S.; Liu, Y.; Wang, Y.; Hao, H.; Buckley, N. J.; Zhang, H.; Wood, I. C.; Gamper, N., Repressor element 1-silencing transcription factor drives the development of chronic pain states. *Pain* **2019,** 160, (10), 2398-2408.
62. Liu, H.; Zeng, L.; Yang, Y.; Guo, C.; Wang, H., Bcl-3: A Double-Edged Sword in Immune Cells and Inflammation. *Front Immunol* **2022,** 13, 847699.
63. Jiang, S.; Li, Z.; Huang, S. J.; Zou, W.; Luo, J. G., IRF7 overexpression alleviates CFA-induced inflammatory pain by inhibiting nuclear factor-κB activation and pro-inflammatory cytokines expression in rats. *Brain Behav Immun* **2024,** 120, 10-20.
64. Sardina, F.; Conte, A.; Paladino, S.; Pierantoni, G. M.; Rinaldo, C., HIPK2 in the physiology of nervous system and its implications in neurological disorders. *Biochim Biophys Acta Mol Cell Res* **2023,** 1870, (5), 119465.
65. Raap, M.; Gierendt, L.; Kreipe, H. H.; Christgen, M., Transcription factor AP-2beta in development, differentiation and tumorigenesis. *Int J Cancer* **2021,** 149, (6), 1221-1227.
66. Wu, H. Y.; Mao, X. F.; Tang, X. Q.; Ali, U.; Apryani, E.; Liu, H.; Li, X. Y.; Wang, Y. X., Spinal interleukin-10 produces antinociception in neuropathy through microglial β-endorphin expression, separated from antineuroinflammation. *Brain Behav Immun* **2018,** 73, 504-519.
67. Li, R.; Shang, J.; Zhou, W.; Jiang, L.; Xie, D.; Tu, G., Overexpression of HIPK2 attenuates spinal cord injury in rats by modulating apoptosis, oxidative stress, and inflammation. *Biomed Pharmacother* **2018,** 103, 127-134.
68. Yang, Y.; Shao, Y.; Dai, Q.; Zhang, Y.; Sun, Y.; Wang, K.; Xu, A., Transcription factor AP-2 Beta, a potential target of repetitive Transspinal magnetic stimulation in spinal cord injury treatment, reduced inflammation and alleviated spinal cord injury. *Exp Neurol* **2025,** 386, 115144.
69. Liang, L. R.; Liu, B.; Cao, S. H.; Zhao, Y. Y.; Zeng, T.; Zhai, M. T.; Fan, Z.; He, D. Y.; Ma, S. X.; Shi, X. T.; Zhang, Y.; Zhang, H., Integrated ribosome and proteome analyses reveal insights into sevoflurane-induced

© 2026 by the author(s). Distributed under a Creative Commons CC BY license.

Preprints.org (www.preprints.org) | NOT PEER-REVIEWED | Posted: 27 April 2026 doi:10.20944/preprints202604.1802.v1

long-term social behavior and cognitive dysfunctions through ADNP inhibition in neonatal mice. *Zool Res* **2024,** 45, (3), 663-678.

70. Medvedeva, Y. A.; Lennartsson, A.; Ehsani, R.; Kulakovskiy, I. V.; Vorontsov, I. E.; Panahandeh, P.; Khimulya, G.; Kasukawa, T.; Drabløs, F., EpiFactors: a comprehensive database of human epigenetic factors and complexes. *Database (Oxford)* **2015,** 2015, bav067.
71. Zhang, W.; Xie, X.; Xiong, X.; Chen, F., HSPA1A Can Alleviate CFA-Induced Inflammatory Pain by Modulating Macrophages. *International journal of molecular sciences* **2025,** 26, (19).
72. Wang, Q.; Zhang, Y.; Du, Q.; Zhao, X.; Wang, W.; Zhai, Q.; Xiang, M., SKF96365 impedes spinal glutamatergic transmission-mediated neuropathic allodynia. *Korean J Physiol Pharmacol* **2023,** 27, (1), 39-48.
73. Hu, J.; Ji, W. J.; Liu, G. Y.; Su, X. H.; Zhu, J. M.; Hong, Y.; Xiong, Y. F.; Zhao, Y. Y.; Li, W. P.; Xie, W., IDO1 modulates pain sensitivity and comorbid anxiety in chronic migraine through microglial activation and synaptic pruning. *Journal of neuroinflammation* **2025,** 22, (1), 42.
74. Wang, J.; Gu, J.; Ma, F.; Wei, Y.; Wang, P.; Yang, S.; Yan, X.; Xiao, Y.; Xing, K.; Lou, A.; Zheng, L.; Cao, T.; Zhu, D.; Li, J.; Zhang, L.; Li, Y.; Chen, T., Melatonin Induces Analgesic Effects through MT(2) Receptor-Mediated Neuroimmune Modulation in the Mice Anterior Cingulate Cortex. *Research (Wash D C)* **2024,** 7, 0493.
75. Li, Z. Z.; Han, W. J.; Sun, Z. C.; Chen, Y.; Sun, J. Y.; Cai, G. H.; Liu, W. N.; Wang, T. Z.; Xie, Y. D.; Mao, H. H.; Wang, F.; Ma, S. B.; Wang, F. D.; Xie, R. G.; Wu, S. X.; Luo, C., Extracellular matrix protein laminin β1 regulates pain sensitivity and anxiodepression-like behaviors in mice. *J Clin Invest* **2021,** 131, (15).
76. Li, Z. Z.; Liu, W. N.; Liu, K. X.; Dou, Z. W.; Zhao, R.; Chen, Y.; Wang, M. M.; Wang, T. Z.; Wang, F.; Han, W. J.; Chu, W. G.; Zheng, X. X.; Xie, R. G.; Yuan, H.; Jiang, X. F.; Sun, X. L.; Luo, C.; Wu, S. X., Cingulate retinoic acid signaling regulates neuropathic pain and comorbid anxiodepression via extracellular matrix homeostasis. *J Clin Invest* **2025,** 135, (17).
77. Yamakawa, W.; Yasukochi, S.; Tsurudome, Y.; Kusunose, N.; Yamaguchi, Y.; Tsuruta, A.; Matsunaga, N.; Ushijima, K.; Koyanagi, S.; Ohdo, S., Suppression of neuropathic pain in the circadian clock-deficient Per2(m/m) mice involves up-regulation of endocannabinoid system. *PNAS Nexus* **2024,** 3, (1), pgad482.
78. Tang, Y. L.; Zhang, Y. Q., [Molecular mechanisms of NMDA receptor-MAPK-CREB pathway underlying the involvement of the anterior cingulate cortex in pain-related aversion]. *Sheng Li Xue Bao* **2017,** 69, (5), 637-646.
79. Zhuo, M., Neural Mechanisms Underlying Anxiety-Chronic Pain Interactions. *Trends in neurosciences* **2016,** 39, (3), 136-145.
80. Li, X. H.; Chen, Q. Y.; Zhuo, M., Neuronal Adenylyl Cyclase Targeting Central Plasticity for the Treatment of Chronic Pain. *Neurotherapeutics : the journal of the American Society for Experimental NeuroTherapeutics* **2020,** 17, (3), 861-873.
81. Cao, H.; Zang, K. K.; Han, M.; Zhao, Z. Q.; Wu, G. C.; Zhang, Y. Q., Inhibition of p38 mitogen-activated protein kinase activation in the rostral anterior cingulate cortex attenuates pain-related negative emotion in rats. *Brain Res Bull* **2014,** 107, 79-88.
82. Galan-Arriero, I.; Avila-Martin, G.; Ferrer-Donato, A.; Gomez-Soriano, J.; Bravo-Esteban, E.; Taylor, J., Oral administration of the p38α MAPK inhibitor, UR13870, inhibits affective pain behavior after spinal cord injury. *Pain* **2014,** 155, (10), 2188-98.
83. Koga, K.; Matsuzaki, Y.; Migita, K.; Shimoyama, S.; Eto, F.; Nakagawa, T.; Matsumoto, T.; Terada, K.; Mishima, K.; Furue, H.; Honda, K., Stimulating muscarinic M(1) receptors in the anterior cingulate cortex reduces mechanical hypersensitivity via GABAergic transmission in nerve injury rats. *Brain research* **2019,** 1704, 187-195.
84. Ortega-Legaspi, J. M.; León-Olea, M.; de Gortari, P.; Amaya, M. I.; Coffeen, U.; Simón-Arceo, K.; Pellicer, F., Expression of muscarinic M1 and M2 receptors in the anterior cingulate cortex associated with neuropathic pain. *Eur J Pain* **2010,** 14, (9), 901-10.
85. Li, X. H.; Matsuura, T.; Xue, M.; Chen, Q. Y.; Liu, R. H.; Lu, J. S.; Shi, W.; Fan, K.; Zhou, Z.; Miao, Z.; Yang, J.; Wei, S.; Wei, F.; Chen, T.; Zhuo, M., Oxytocin in the anterior cingulate cortex attenuates neuropathic pain and emotional anxiety by inhibiting presynaptic long-term potentiation. *Cell reports* **2021,** 36, (3), 109411.

© 2026 by the author(s). Distributed under a Creative Commons CC BY license.

Preprints.org (www.preprints.org) | NOT PEER-REVIEWED | Posted: 27 April 2026 doi:10.20944/preprints202604.1802.v1

86. Shi, C. N.; Wu, X. M.; Gao, Y. Z.; Ma, D. Q.; Yang, J. J.; Ji, M. H., Oxytocin attenuates neuroinflammation-induced anxiety through restoration of excitation and inhibition balance in the anterior cingulate cortex in mice. *J Affect Disord* **2024,** 362, 341-355.
87. Dityatev, A.; Schachner, M.; Sonderegger, P., The dual role of the extracellular matrix in synaptic plasticity and homeostasis. *Nature reviews. Neuroscience* **2010,** 11, (11), 735-46.
88. Ji, R. R.; Nackley, A.; Huh, Y.; Terrando, N.; Maixner, W., Neuroinflammation and Central Sensitization in Chronic and Widespread Pain. *Anesthesiology* **2018,** 129, (2), 343-366.
89. Wei, N.; Guo, Z.; Qiu, M.; Ye, R.; Shao, X.; Liang, Y.; Liu, B.; Fang, J.; Fang, J.; Du, J., Astrocyte Activation in the ACC Contributes to Comorbid Anxiety in Chronic Inflammatory Pain and Involves in The Excitation-Inhibition Imbalance. *Molecular neurobiology* **2024,** 61, (9), 6934-6949.
90. Duan, Y. W.; Chen, S. X.; Li, Q. Y.; Zang, Y., Neuroimmune Mechanisms Underlying Neuropathic Pain: The Potential Role of TNF-α-Necroptosis Pathway. *International journal of molecular sciences* **2022,** 23, (13).
91. Jia, D.; Gao, G. D.; Liu, Y.; He, S. M.; Zhang, X. N.; Zhang, Y. F.; Zhao, M. G., TNF-alpha involves in altered prefrontal synaptic transmission in mice with persistent inflammatory pain. *Neuroscience letters* **2007,** 415, (1), 1-5.
92. Jiang, A. J.; Wei, H. R.; Chu, S.; Wang, M.; Yan, J.; Song, X. L.; Xu, T. L.; Zhang, Z.; Jin, Y.; Wang, W., Upregulation of Acid-Sensing Ion Channel 1a in the Anterior Cingulate Cortex by TNF-α/NF-κB Pathway Contributes to Diabetes-Related Pain. *Diabetes* **2025,** 74, (6), 1007-1020.
93. Yao, P. W.; Wang, S. K.; Chen, S. X.; Xin, W. J.; Liu, X. G.; Zang, Y., Upregulation of tumor necrosis factor-alpha in the anterior cingulate cortex contributes to neuropathic pain and pain-associated aversion. *Neurobiology of disease* **2019,** 130, 104456.
94. Chou, C. W.; Wong, G. T.; Lim, G.; Wang, S.; Irwin, M. G.; Mao, J., Spatiotemporal pattern of concurrent spinal and supraspinal NF-κB expression after peripheral nerve injury. *J Pain* **2011,** 12, (1), 13-21.
95. Dai, J. H.; Xu, Z. H.; Li, Q. L.; Huang, J.; Niu, Z.; Zhang, C. H.; Hu, S.; Sun, R.; Li, Y. C., TRIM14-NF-κB pathway in the anterior cingulate cortex modulates comorbid depressive symptoms in chronic pain. *Molecular pain* **2025,** 21, 17448069251335503.
96. Brezic, N.; Gligorevic, S.; Sic, A.; Knezevic, N. N., Protein Misfolding and Aggregation as a Mechanistic Link Between Chronic Pain and Neurodegenerative Diseases. *Curr Issues Mol Biol* **2025,** 47, (4).
97. Reichling, D. B.; Levine, J. D., Pain and death: neurodegenerative disease mechanisms in the nociceptor. *Ann Neurol* **2011,** 69, (1), 13-21.
98. Tian, Z.; Zhang, Q.; Wang, L.; Li, M.; Li, T.; Wang, Y.; Cao, Z.; Jiang, X.; Luo, P., Progress in the mechanisms of pain associated with neurodegenerative diseases. *Ageing Res Rev* **2024,** 102, 102579.
99. Deneubourg, C.; Ramm, M.; Smith, L. J.; Baron, O.; Singh, K.; Byrne, S. C.; Duchen, M. R.; Gautel, M.; Eskelinen, E. L.; Fanto, M.; Jungbluth, H., The spectrum of neurodevelopmental, neuromuscular and neurodegenerative disorders due to defective autophagy. *Autophagy* **2022,** 18, (3), 496-517.
100. Liu, X.; Zhu, M.; Ju, Y.; Li, A.; Sun, X., Autophagy dysfunction in neuropathic pain. *Neuropeptides* **2019,** 75, 41-48.
101. Liao, M. F.; Lu, K. T.; Hsu, J. L.; Lee, C. H.; Cheng, M. Y.; Ro, L. S., The Role of Autophagy and Apoptosis in Neuropathic Pain Formation. *International journal of molecular sciences* **2022,** 23, (5).
102. Zhang, E.; Yi, M. H.; Ko, Y.; Kim, H. W.; Seo, J. H.; Lee, Y. H.; Lee, W.; Kim, D. W., Expression of LC3 and Beclin 1 in the spinal dorsal horn following spinal nerve ligation-induced neuropathic pain. *Brain research* **2013,** 1519, 31-9.
103. Yin, Y.; Yi, M. H.; Kim, D. W., Impaired Autophagy of GABAergic Interneurons in Neuropathic Pain. *Pain research & management* **2018,** 2018, 9185368.
104. Shi, G.; Shi, J.; Liu, K.; Liu, N.; Wang, Y.; Fu, Z.; Ding, J.; Jia, L.; Yuan, W., Increased miR-195 aggravates neuropathic pain by inhibiting autophagy following peripheral nerve injury. *Glia* **2013,** 61, (4), 504-12.
105. Meng, X. L.; Fu, P.; Wang, L.; Yang, X.; Hong, G.; Zhao, X.; Lao, J., Increased EZH2 Levels in Anterior Cingulate Cortex Microglia Aggravate Neuropathic Pain by Inhibiting Autophagy Following Brachial Plexus Avulsion in Rats. *Neuroscience bulletin* **2020,** 36, (7), 793-805.
106. Fu, S.; Sun, H.; Wang, J.; Gao, S.; Zhu, L.; Cui, K.; Liu, S.; Qi, X.; Guan, R.; Fan, X.; Liu, Q.; Chen, W.; Su, L.; Cui, S.; Liao, F.; Liu, F.; Wong, C. C. L.; Yi, M.; Wan, Y., Impaired neuronal macroautophagy in the prelimbic

© 2026 by the author(s). Distributed under a Creative Commons CC BY license.

Preprints.org (www.preprints.org) | NOT PEER-REVIEWED | Posted: 27 April 2026 doi:10.20944/preprints202604.1802.v1

cortex contributes to comorbid anxiety-like behaviors in rats with chronic neuropathic pain. *Autophagy* **2024,** 20, (7), 1559-1576.

107. Lin, J.; Zhang, W.; Wang, S.; Wang, C.; Zhang, R.; Yang, Y.; Zhou, C.; Zhang, L.; Tang, P.; Liu, J.; Jin, X.; Ma, Y., Astragalin inhibits neuronal excitability and activates neuronal autophagy in the ACC and LH of CFA mice to alleviate inflammatory pain and pain-related emotions. *Int Immunopharmacol* **2025,** 148, 114115.
108. Xu, Y.; Xing, F.; Wei, X.; Wang, X.; Shi, X.; Wang, Z.; Xing, N.; Yuan, J.; Li, Z.; Zhang, W., TMEM251 loss-induced autophagy dysfunction in the anterior cingulate cortex contributes to chronic postoperative pain. *EMBO Rep* **2025**.
109. Doyle, T. M.; Salvemini, D., Mini-Review: Mitochondrial dysfunction and chemotherapy-induced neuropathic pain. *Neuroscience letters* **2021,** 760, 136087.
110. Bennett, G. J.; Doyle, T.; Salvemini, D., Mitotoxicity in distal symmetrical sensory peripheral neuropathies. *Nature reviews. Neurology* **2014,** 10, (6), 326-36.
111. Dai, C. Q.; Guo, Y.; Chu, X. Y., Neuropathic Pain: the Dysfunction of Drp1, Mitochondria, and ROS Homeostasis. *Neurotoxicity research* **2020,** 38, (3), 553-563.
112. Huang, Z.; Xiao, P. Y.; Chen, J. Y.; Zeng, Q.; Huang, B. X.; Yu, J.; Liao, S. J., Mammalian Sterile 20-Like Kinase 1 Mediates Neuropathic Pain Associated with Its Effects on Regulating Mitophagy in Schwann Cells. *Oxidative medicine and cellular longevity* **2022,** 2022, 3458283.
113. Shao, S.; Xu, C. B.; Chen, C. J.; Shi, G. N.; Guo, Q. L.; Zhou, Y.; Wei, Y. Z.; Wu, L.; Shi, J. G.; Zhang, T. T., Divanillyl sulfone suppresses NLRP3 inflammasome activation via inducing mitophagy to ameliorate chronic neuropathic pain in mice. *Journal of neuroinflammation* **2021,** 18, (1), 142.
114. Li, C.; Wang, X. G.; Yang, S.; Lyu, Y. H.; Gao, X. J.; Cao, J.; Zang, W. D., [Treadmill exercise alleviates neuropathic pain by regulating mitophagy of the anterior cingulate cortex in rats]. *Sheng Li Xue Bao* **2023,** 75, (2), 160-170.
115. Vilar, E.; Perez-Garcia, J.; Tabernero, J., Pushing the envelope in the mTOR pathway: the second generation of inhibitors. *Mol Cancer Ther* **2011,** 10, (3), 395-403.
116. Liu, S.; Zhu, R.; Zhang, Y.; Jiang, Z.; Chen, Y.; Song, Q.; Wang, F., Targeting PI3K-mTOR signaling in the anterior cingulate cortex improves emotional behavior, and locomotor activity in rats with bone cancer pain. *Ann Med Surg (Lond)* **2025,** 87, (4), 1985-1994.
117. Burish, M. J.; Chen, Z.; Yoo, S. H., Emerging relevance of circadian rhythms in headaches and neuropathic pain. *Acta Physiol (Oxf)* **2019,** 225, (1), e13161.
118. Bumgarner, J. R.; Walker, W. H., 2nd; Nelson, R. J., Circadian rhythms and pain. *Neurosci Biobehav Rev* **2021,** 129, 296-306.
119. Logan, R. W.; Xue, X.; Ketchesin, K. D.; Hoffman, G.; Roussos, P.; Tseng, G.; McClung, C. A.; Seney, M. L., Sex Differences in Molecular Rhythms in the Human Cortex. *Biological psychiatry* **2022,** 91, (1), 152-162.
120. Bunney, B. G.; Li, J. Z.; Walsh, D. M.; Stein, R.; Vawter, M. P.; Cartagena, P.; Barchas, J. D.; Schatzberg, A. F.; Myers, R. M.; Watson, S. J.; Akil, H.; Bunney, W. E., Circadian dysregulation of clock genes: clues to rapid treatments in major depressive disorder. *Molecular psychiatry* **2015,** 20, (1), 48-55.

Disclaimer/Publisher's Note: The statements, opinions and data contained in all publications are solely those of the individual author(s) and contributor(s) and not of MDPI and/or the editor(s). MDPI and/or the editor(s) disclaim responsibility for any injury to people or property resulting from any ideas, methods, instructions or products referred to in the content.

© 2026 by the author(s). Distributed under a Creative Commons CC BY license.